Are Headforms a Poor Surrogate for Helmet Fit?

## Kristie Liu

Department of Kinesiology and Physical Education, Faculty of Education,
McGill University
Montreal, Quebec, Canada

February 2018

A thesis submitted to McGill University in partial fulfillment of the requirements of the degree of Master of Science Kinesiology and Physical Education

#### Abstract:

International standards organizations require ice hockey helmets to be impact tested while mounted to a surrogate headform, with anthropometrics of a 50<sup>th</sup> percentile male. However, human head shapes are not identical, nor are there consistent guidelines for fitting a helmet to the ordinary user. The interaction of head shape and helmet fit matters in helmet safety: the contact area between a headform and helmet interior has been identified as a critical determinant of protection afforded by a helmet. The objective of this study was to compare quantitative measures of helmet fit between an adult male sample and the three 50<sup>th</sup> percentile male headforms (HFs). The following study recruited 42 adult male participants who wore a medium sized ice hockey helmet in an attempt to compare their quantitative helmet fit to those of three 50<sup>th</sup> percentile adult male HFs. Through 3D modeling, fit was quantified by assessing dimensional differences in two transverse cross-sectional planes of the head, and by using Principal Component Analysis (PCA) to determine the largest components of fit. Significant differences were found between the HFs and the participant's heads in anthropometrics and dimensional differences. The HFs were smaller than the participants' heads, demonstrating average gapping with the interior of the helmet. The principal components of fit extracted included medial-lateral warping, gapping/compression at the rear aspect of the helmet-head interface, and general congruence of the head shape to the helmet liner. These findings demonstrated incongruence in helmet fit between surrogate headforms and ordinary users.

#### Résumé

Les organisations des normes internationales exigent que les casques de hockey sur glace soient soumis à un test d'impact lorsqu'ils sont montés sur une fausse forme de tête (FFT), avec les anthropométries d'un homme du 50ème centile. Cependant, les formes de tête humaines ne sont pas uniformes, donc il n'y a pas de standard cohérent pour l'ajustement d'un casque pour l'utilisateur tous les jours. L'interaction de la tête et l'ajustement du casque sont importants pour raison de sécurité: la région de contact entre une fausse forme de tête et l'intérieur du casque a été identifié comme un déterminant essentiel de la protection offerte par un casque. L'objectif de cette étude était de comparer des mesures quantitatives de l'ajustement du casque de hockey sur glace contre un échantillon d'adultes mâles et trois fausses formes de tête (FFT) aussi d'adultes mâles du 50ème centile. Cette étude a recruté 42 participants qui portaient un casque de hockey de grandeur moyen dans le but de comparer leur ajustement personel du casque à celui de trois FFT d'adultes mâles du 50ème centile. Avec l'aide de modélisation 3D, l'ajustement du casque a été quantifié en évaluant les différences dimensionnelles dans deux sections transversaux de la tête. De plus, la technique de Principal Component Analysis (PCA) a été utilisé pour déterminer les plus grands composants de l'ajustement du casque. Des différences ont été trouvés entre les FFT et les têtes des participants dans l'anthropométrie et les différences dimensionnelles. Les FFT étaient plus petites que les têtes de participants, démontrant un écart avec l'intérieur du casque. Les PCA du casque comprenaient le gauchissement médial-latéral, écart/compression à l'arrière de l'interface casque-tête et la congruence générale de la tête au matériel de l'intérieur du casque. Ces mesures démontrent une incongruence entre les FFT et l'ajustement du casque de les utilisateurs réels.

# Contents

| Abstract:  | 3    |
|--|------|
| Résumé   | 4    |
| Acknowledgements   | 7    |
| Contribution of Authors                                      | 8    |
| 1. Introduction  | 9    |
| 2. Literature Review   |      |
| 2.1 Concussion   |      |
| 2.2 Helmets  |      |
| 2.3 Hockey helmet impact testing                             |      |
| 2.4 Helmet Fit and Head Anthropometrics                      | 17   |
| 2.5 Photogrammetry   | 18   |
| 3. Manuscript  | 20   |
| 3.1 Abstract   | 21   |
| 3.2 Introduction   | 22   |
| 3.3 Methods  | 25   |
| 3.3.1 Ethics   | 25   |
| 3.3.2 Participants   | 25   |
| 3.3.3 Helmet   | 26   |
| 3.3.4 Equipment and Software                                 | 26   |
| 3.3.5 Protocol   | 27   |
| 3.3.6 Participant Testing Protocol                           | 27   |
| 3.3.7 Helmet on Head (Intermediate) Scans                    | 30   |
| 3.3.8 Create 3D Helmet Models                                | 31   |
| 3.3.9 Data Processing  | 31   |
| 3.3.10 Statistical analysis                                  | 34   |
| 3.4 Results  | 35   |
| 3.4.1 Head Shape and Headform Anthropometrics                | 35   |
| 3.4.2 Helmet Dimensional Differences                         | 38   |
| 3.4.3 Principal Component Analysis of Dimensional Difference | es40 |
| 3.4.4 M_5 sub-analysis                                       | 47   |
| 3.4.4.1 Helmet Dimensional Differences                       | 50   |
| 3.4.4.2 Headform PC ranks                                    | 51   |

| 3.5 Discussion  | 52 |
|---|----|
| 3.5.1 Helmet referenced slice   | 52 |
| 3.5.2 Standard impact sites   | 53 |
| 3.5.3 Dimensional Differences   | 54 |
| 3.5.4 Principal Component Analysis of Helmet-to-Head Fit: Dimension Differences Variance Explained  | 55 |
| 3.5.5 M_5 Sub-analysis  | 57 |
| 3.5.6 Implications  | 58 |
| 3.5.7 Limitations   | 58 |
| 3.5.8 Future Directions   | 59 |
| 3.6 Conclusion  | 60 |
| 1 Helmet referenced slice       52         2 Standard impact sites       53         3 Dimensional Differences       54         4 Principal Component Analysis of Helmet-to-Head Fit: Dimension Differences riance Explained       55         55 M_5 Sub-analysis       57         6 Implications       58         7 Limitations       58         8 Future Directions       59         Conclusion       60         Acknowledgements       60         clusions       61         erences       62         endices       66         ndix A: Consent form       66         ndix B: Participant Demographics and Anthropometrics       69 |    |
| 4. Conclusions  | 61 |
| 5. References   | 62 |
| 6. Appendices   | 66 |
| Appendix A: Consent form  | 66 |
| Appendix B: Participant Demographics and Anthropometrics  |    |
| Appendix C: Helmet Fit Questionnaire  | 70 |

### Acknowledgements

I would like to begin by thanking my thesis supervisor, Dr. David Pearsall. Without your insight, feedback, and expertise, this project would not have been feasible. I am incredibly grateful for the opportunity to work, learn, and grow in the Ice Hockey Research Group under your supervision. To my thesis advisory committee, including my co-supervisor Dr. Shawn Robbins, and Dr. Caroline Paquette, thank you for all of your guidance and feedback on this thesis. Thank you specifically to Dr. Robbins for your expertise on Principal Component Analysis; your advice throughout this project was tremendously appreciated.

To Dan Aponte, thank you for taking me under your wing, and for all of your efforts that went into the H.E.A.D. project. You brought me up to speed for the second iteration of this project and helped me become a better researcher. I wish you the best of luck as you continue on your path towards becoming Dr. Dan. To Dave Greencorn, thank you for your endless patience in helping me follow in your footsteps. Your legacy on this project was essential in the completion of this thesis.

To Aleks Budarick, Dan Boucher, and Phil Renaud, thank you for creating the great atmosphere in the lab. You guys welcomed me to the Ice Hockey Research Group, and I wish only the best for your future endeavours. To Aiden Hallihan and Brian McPhee, thank you for being on this journey since Day 1. To everyone in the KPE department, thank you for making grad school such a fun and supportive environment. To my lacrosse families, thank you for your encouragement on and off the field.

Lastly, I would like to thank my family for supporting me from the very beginning of this Master's thesis. I would not be where I am today without your constant love and encouragement; thank you for always being there for me and helping me accomplish my goals.

### **Contribution of Authors**

Kristie Liu, MSc candidate, McGill University, was actively involved in the data collection process, and was responsible for the data processing, analysis, and writing of this thesis. David J. Pearsall, PhD, Associate Professor, Department of Kinesiology and Physical Education, McGill University, contributed to the research design, protocol, and planned analysis as the candidate's supervisor. The thesis advisory committee consisting of the candidate's cosupervisor, Shawn Robbins, PhD, Assistant Professor, School of Physical and Occupational Therapy, McGill University, and Caroline Paquette, PhD, Assistant Professor, Department of Kinesiology and Physical Education, McGill University, contributed to the research design and protocol. Dr. Robbins provided guidance on the principal component analysis for the data of this thesis.

Daniel I. Aponte, PhD Candidate, McGill University, assisted in the research design and protocol, recruitment, and data collection for this study. David J. Greencorn, MSc, McGill University, assisted in the research design and protocol, and developed custom MATLAB scripts used for data processing.

#### 1. Introduction

Ice hockey is a popular recreational and competitive winter sport; however, the high incidence of sport related concussions is of concern [1]. For instance, in Canadian minor hockey, concussion is the most common specific injury type [2]. At the collegiate level, concussion is the most common injury in women's ice hockey, and second most common for men [3,4]. Ice hockey helmets were adopted as required equipment in competitive play in the 1980's to reduce the prevalence of head injuries, particularly skull fractures [5]. In order for ice hockey helmet models to be certified for commercial sale, sample helmets must pass a standardized series of controlled impact drop tests of helmet mounted on surrogate headforms [6–8].

According to most international testing standards, for medium sized ice hockey helmets, impact tests are performed on 50th percentile adult male surrogate headforms (circumference of 575mm about the Reference Plane) [8]. Peak linear acceleration has been the most common measurement criterion to be assessed for impact protection in the sports industry. The established pass/fail criterion for helmets standards are between 250-300g, believed to be the threshold for skull fracture; however, the extent to which certified helmets can reduce the incidence of concussion has been limited [9]. Notably, recent research has implicated high rotational accelerations as an important concussion risk factor [10,11], though to date no current hockey helmet standard includes rotational acceleration due to the complexity in defining repeatable testing methodology and criterion thresholds [9].

In addition to the above, on an elementary level, all standards state proper helmet fit is essential for helmet function; yet, other than a defined area of coverage and retention stability, a quantitative definition of helmet-to-head fit is lacking. However, recent evidence suggests that helmet-to-head size differences affect impact behaviour. In a study on motorcycle helmets, peak acceleration and Head Injury Criterion were measured using finite element modeling under two

conditions: first, different combinations of an allometrically scaled Hybrid III 50<sup>th</sup> percentile headform (at 0.8, 0.9, and 1.1 scale) with the original helmet; and second, the baseline Hybrid III headform with the allometrically scaled helmet (at 1.1 and 1.2 scale) [12]. These scaling factors, typically within a given helmet-to-head size pairing, substantially altered head impact responses. The authors stated that contact area between the interface of the headform and helmet liner was a critical determinant of protection afforded by the helmet to the headform. By extension, variations in the user's head shape proportions may further alter helmet fit and its protective capacity.

Similarly, surrogate head shape proportions may matter in terms of standardized testing protocols. For instance, different surrogate headform shapes used by NOCSAE, ASTM, ISO/CEN and CSA vary substantially on visual inspection. Further, the Hybrid III headform, developed within the automotive industry for crash test dummies, varies distinctively in shape and size from these other headforms [8,13]. The Hybrid III headform and neck combinations have been adopted by various research groups, given the multi-triaxial accelerometer configuration offers angular acceleration estimates. However, the Hybrid III headform was designed solely on the average cranial measurements of a collection of 16 Caucasian male adult skulls [14]. Likewise, the NOCSAE headform was designed based on average anthropometrics of 13 cadaver heads within the size range of the most popular football helmet size [15]. Between these two headforms substantial differences were noted in the back cranial regions [13].

The use of anthropometric averages to generalize a population should be done with caution. For example, the classic study examining the average of ten physical dimensions of over 4000 pilots revealed no single subject fell within the average range of all measured dimensions [16]. Thus, designing for an "average individual" risks being unsatisfactory for all users [16].

This fallacy is highlighted by a recent study, where differences in head shape were observed between a sample of adult males and standard headforms with the anthropometrics of a 50<sup>th</sup> percentile adult male [17]. For instance, a study of bicycle helmet fit demonstrated that female and Asian helmet users had lower fit scores than male and Caucasian users, respectively, for a given size of helmet [18]. Furthermore, using two large datasets of Caucasian and Chinese head shapes obtained by using 3D laser scanning technology, Ball et al. revealed significant variations in size, shape, and proportion between the two demographics [19].

Hence, the rationale for this study is to address a potential disconnect between standard headforms and actual users with regards to helmet fit. Using the protocol developed by Greencorn [20], this study will quantitatively compare helmet fit between headforms and a sample of adult males. We hypothesize differences will be observed in the way helmets fit on headforms and on humans, in terms of both the gapping and compression of the foam liner at the helmet-to-head interface. Further, it is expected distinct head-helmet fit profiles, in terms of regional locations of relative gapping and compression of the helmet liner, will be observed.

In the following text, an expanded description of relevant literature related to concussion, helmet testing standards, and 3D shape analysis techniques will be reviewed. This background knowledge will discuss in greater detail the issues and challenges surrounding head protection in sport.

## 2. Literature Review

Previous research related to head protection in sport will be presented in the following sections. This will include an overview of concussion. Subsequently, the progression of hockey helmets from their origins to their current state will be described. This will be followed by a summary of the impact testing used to certify hockey helmets. Next, helmet fit and head anthropometrics will be integrated. Lastly, photogrammetry, the method of 3D model acquisition, will be explained.

### 2.1 Concussion

Head injuries can be categorized into two broad classes: open (i.e. penetrating) and closed injuries (i.e. non-penetrating), defined by a broken or intact skull, respectively [21]. Open head injury is caused by focalized stress on the skull induced by collision with a sharp objects, resulting in skull fracture [21]. Conversely, closed head injuries typically occur as a result of blunt forces, leaving the skull intact [21]. A prime example of a closed head injury is a concussion, a topic of public concern.

Concussion is a category of mild traumatic brain injury (mTBI), and is currently defined as a "complex pathophysiological process affecting the brain, induced by traumatic biomechanical forces" [22]. Additional features include 1) causation by either a direct impact to the head, face, neck or another part of the body where impulsive force is transmitted to the head; 2) the rapid onset of short-term neurological impairment that resolves spontaneously; 3) acute symptoms reflecting functional disturbance rather than structural damage; 4) the presentation of a graded set of symptoms, that may or may not involve loss of consciousness, and typically resolve sequentially; and, 5) the absence of abnormality on standard structural neuroimaging [22]. Symptoms of a concussive head injury may include physical signs (e.g. loss of consciousness, amnesia), behavioral changes (e.g. irritability), cognitive impairment (e.g. slowed

reaction times), sleep disturbance, somatic symptoms (e.g. headaches), cognitive symptoms (e.g. feeling in a fog), or emotional symptoms (e.g. emotional lability) [22]. The majority of concussions (80-90%) resolve within a 7-10 day period; however, this period of recovery may be longer for children and adolescents [22].

Concussion is not a visible injury, thus a large part of injury recognition is dependent on an individual's self-reporting of symptoms. Evaluation of an athlete with a suspected concussion involves cognitive assessment. One such evaluation is the Sport Concussion Assessment Tool (SCAT2), which represents a standardized method of evaluating individuals after sustaining a concussion from sport [22-24]. Increased awareness and knowledge of concussion is crucial to the assessment and management of this injury. Concussion awareness initiatives have contributed to the increasing number of sports-related concussion reported in the NCAA [23]; however, there is a general consensus among sports medicine professionals that the true rate of concussion in sports is still higher than the incidence of recorded injury [25,26]. This dilemma may be further complicated by an athlete's naivety and/or tendency to under report symptoms in an attempt to expedite return to play [25]. Consequently, significant concerns regarding second impact syndrome have been prompted. This condition manifests when an athlete who has sustained a head injury, often a concussion, experiences a second head impact prior to the resolution of the initial injury [27]. While the exact rate of mortality associated with second impact syndrome cannot be determined due to undiagnosed and unreported concussion, it has been implicated in the deaths of multiple young athletes [28]. In an effort to reduce premature return to play, a graded six step protocol has been developed to assist athletes, medical professionals, parents, and coaches in making safe return to sport decisions [22].

The elevated profile of concussion in sports and healthcare discourse has led to increased public awareness and concern. It is estimated between 1.6 and 3.8 million sports related concussions occur annually in the United Sates, and at least 5.3 million Americans are living with long-term disability associated with a traumatic brain injury [29]. Due to the large number of youths and adolescents participating in sport, these age groups account for the majority of sport-related concussions [30]. In high school athletics, an estimated 300,000 head injuries occur annually, with 90% of these injuries being concussion [31]. In a study on Canadian minor hockey players, concussion was the most common injury type, accounting for 18% of all reported injuries [32]. In collegiate level ice hockey, concussion is the most common injury in women and second for men [3,4].

The prevalence of concussion in youth has prompted further research on the effects of this injury on the developing brain, with some startling findings. For example, the rate of concussion in high school athletes has been observed to be greater than that of older athletes within the same sport [33]. Furthermore, high school athletes tend to have poorer outcomes with concussion, demonstrating significant memory impairment for a much longer duration than college athletes with concussion [34]. In a study comparing concussion recovery of National Football League (NFL) and high school athletes, all NFL athletes returned to baseline neuropsychological performance within a week of injury; high school athletes, however, displayed neuropsychological deficits beyond the seven day follow-up period [35].

The biomechanical forces induced by a head impact are both translational and rotational. It has been estimated the peak linear acceleration of the head at 66 G, 82G, and 106G would result in a 25%, 50%, and 80% probability of concussion, respectively [36]. Similarly, it has been estimated maximal rotational accelerations of the head at  $4.6 \times 10^3$ ,  $5.9 \times 10^3$ , and  $7.9 \times 10^3$ 

rad/s<sup>2</sup> would have a 25%, 50%, and 80% probability of concussion, respectively [36]. Some studies even suggest rotational accelerations may be the primary mechanism of concussion, due to shearing of brain tissue [10,37]. This is thought to be explained by the inherent physical characteristics of brain tissue, demonstrating very low resistance to shear forces associated with rotation, but higher resistance to compressive forces associated with translation [10,38,39].

#### 2.2 Helmets

Clement and Jones [5] detail the history of helmets in hockey. In the early 1950s, hockey players were headgear composed of felt-lined leather held together by straps. These were soon replaced by lightweight protective headgear, developed through advances in modern plastics and the use of injection-molding techniques. By the early 1970s, the prevalent helmet construction was dual-component: an outer plastic shell manufactured through injection and interior foam to absorb energy and provide a comfortable fit.

The International Organization for Standardization (ISO) standard was published in 2003, as a single international standard for use to certify hockey helmets. Currently, ISO is one of four standards for ice hockey (refer to "Helmet Impact Testing" section below). Hockey helmet standards were developed using the same research evidence used to create American football helmet standards. As a result, the standards used similar methodologies and criteria, while accounting for the unique risks involved each sport individually. Nearly all hockey leagues in North America adopted helmets as required equipment following the death of Bill Masterton, a professional hockey player, in 1968 from a head injury. The National Hockey League was the last league to implement the required use of a certified helmet in 1979 [5].

Hockey helmets are currently designed for multiple impact use by combining a semi-rigid outer shell and an inner foam liner [9,40]. The outer shell functions by dispersing the energy of an impact over a larger surface area, thus resisting puncture and focal injuries [9]. Outer shells

are composed of polycarbonates, fiber reinforced, or injected polyethylene plastics [9]. The foam liner of a hockey helmet is the primary energy absorbing element; these foams are primarily made of expanded polypropylene, expanded polyethylene, vinyl nitrile, or cross-linked polyethylene foams [9]. These recoverable elastic foams (i.e. return to original shape) are intended for multiple impacts, and dissipate energy through elastic deformation of air cells, without structural damage to the cell walls [41,42]. The impact absorption capabilities of helmet liners can be optimized by balancing the thickness and density of the foam [41–43].

For the purpose of constructing an effective head protection device, different mathematical models have been developed to better understand head injury mechanisms. For example, the Wayne State Tolerance Curve (WSTC) was created as a means of defining the tolerance of the human skull to various impacts [44]. Tests on human cadavers and dogs produced pressure-time and acceleration-time tolerance curves, demonstrating tolerance to higher magnitude translations can be endured for short durations and low magnitude translations for longer durations [44]. Further empirical models were created, such as the Gadd Severity Index (GSI) and Head Injury Criterion (HIC), developed from the WSTC for the helmet and motorsport industries, respectively [45,46]. These injury tolerance criteria associate peak resultant linear head acceleration with severe head injury, where injury criterion is the onset of skull fracture [44]. As such, linear acceleration is currently the most common variable used for certification of helmets in the sports industry; the established pass/fail criteria for helmet standards are approximately 250-300g, equal to the threshold for skull fracture [9]. Linear acceleration-based injury criteria have been effective in the development of safer helmets, in terms of reducing traumatic skull fractures in sports; however, these helmets have had limited

effect on reducing incidence of concussion [9]. As of late, increased attention has been placed on including rotational acceleration as an important metric of concussive injury [10,11].

## 2.3 Hockey helmet impact testing

Hockey leagues require players to wear helmets certified by the governing agency specific to the country where games are played. Several standards for hockey helmets have been created internationally. These are the Canadian Standards Association (CSA) [47], American Society for Testing and Materials (ASTM) [48], the Comité European de Normalisation (CEN) [49], and the International Organization for Standardization (ISO) [50]. Each standard has slightly different specifications, including the headform used, pass/fail criterion, impact locations, impact velocities, and testing apparatus used [8]. In order to be certified, helmets must reduce peak linear acceleration below thresholds based on kinematic research on skull fracture [9].

Though recent studies have implicated rotational acceleration as an important contributing factor to concussion, this relationship is ill-defined given the high inter-subject variability between insult and symptoms; hence, no official helmet standard uses rotational acceleration as a measure of helmet performance [51]. The Summation of Tests for the Analysis of Risk (STAR) is a newly developed hockey helmet evaluation methodology, incorporating both linear and rotational acceleration components, to rate helmet performance based on the ability to reduce the risk of concussion [52]; however, STAR is not sanctioned by any safety nor sport organization body.

### 2.4 Helmet Fit and Head Anthropometrics

Helmet fit has been identified as an important factor affecting helmet function, yet it has only recently been investigated quantitatively [12,53]. As demonstrated through finite element modeling, the fit conditions of different headform sizes to a particular helmet greatly affect the

impact absorption capacity of the helmet [12]. Helmet fit is not a trivial issue, as individuals with similar head circumference can have different preference of hockey helmet models and adjustment settings [20]. Furthermore, subjective fit scores are poorly related to a quantitative measure of the distance between helmet liner and head surface perimeters [20].

Helmets of different size ranges (S, M, L based on transverse head circumferences) are tested using surrogate headforms with average geometric dimensions of 50th percentile males [8,9]. Compiled anthropometric data has typically been acquired from a Caucasian or European population [54]. It should be noted, however, that the congruence of headforms to the user population has yet to be investigated or validated. The latter is of concern; for example, a recently developed metric for bicycle helmet fit, based on 3D head-helmet contact area, revealed female and Asian helmet wearers had poorer fit scores than male and Caucasian users, respectively [18]. Further, in a study using 3D anthropometric surveys to compare the head shapes of Caucasian (n=4000) and Chinese (n=2000), significant variations were discovered. From the comparison of the adult male samples, differences in size, shape (i.e. round versus oval), and proportions were observed [19][19]. The findings of this study demonstrate non-uniformity in head shape across ethnicities [19]. Given that 3D scanning technology has become practical, inexpensive and rapid, further study using this technology to investigate helmet design fit ergonomics is feasible.

From the above review, the goal of designing ice hockey helmets to reduce concussion prevalence and severity remains an elusive goal as many factors must be considered. The goal of this study is to address one factor: ice hockey helmet-to-head fit parameters.

## 2.5 Photogrammetry

Different technologies are available to acquire 3D models: from medical imaging technologies such as Computed Tomography [55] and Magnetic Resonance Imaging [56], to

surface shape laser scanning [19,57,58] to create 3D head volume shapes. Another option is photogrammetry [20,59], which has become more affordable and portable. Photogrammetry is the art and science of taking measurements from photographs to reconstruct objects or scenes in 2D or 3D [60]. Close range photogrammetry applies to objects up to 200m in size, and can be used to generate textured 3D models of objects or scenes [60]. The digital processing of imagebased 3D models begins with camera calibration and image orientation: these steps assist with the identification and digital alignment of shared features visible in the images [61]. Identification of these "tie points" (i.e. shared features) can be performed manually by an expert operator; however, with increases in computational power and advances in computer vision, commercially available software solutions (e.g. PhotoScan, Agisoft; ReCap, AutoDesk) have been developed for the automated extraction of consistent and redundant sets of tie points from markerless images [61]. Following image orientation, surface measurement and feature extraction are the next steps in the 3D reconstruction and modeling process [61]. Once the software has solved for the camera location of each photograph, in a first pass, the scene or object is digitally reconstructed as a sparse point cloud of common-features [61]. The second phase of point cloud generation uses additional information from the photographs to fill gaps in the sparse point cloud to generate a dense point cloud of the scene or object. The dense point cloud can then be converted to a triangular mesh, complete with true-to-life textures, a feature that sets photogrammetry apart from other 3D scanning technologies [17,20]. Photogrammetry has been successfully used to quantitatively assess helmet fit [20], and thus was implemented for the 3D acquisition of the present study.

| 3. Manuscript  |
|--|
| Are Headforms a Poor Surrogate for Ice Hockey Helmet Fit?  |
| Kristie Liu <sup>1</sup> , Daniel I. Aponte <sup>1</sup> , David J. Greencorn <sup>1</sup> , Shawn M. Robbins <sup>2</sup> , David J Pearsall <sup>1</sup> |
|  |
|  |

<sup>&</sup>lt;sup>1</sup> Department of Kinesiology and Physical Education, McGill University, Montreal, Quebec, Canada

<sup>&</sup>lt;sup>2</sup> School of Physical and Occupational Therapy, McGill University, Montreal, Quebec, Canada

#### 3.1 Abstract

International standards organizations require ice hockey helmets to be impact tested while mounted to a surrogate headform, with anthropometrics of a 50<sup>th</sup> percentile male. However, human head shapes are not identical, nor are there consistent guidelines for fitting a helmet to the ordinary user. The interaction of head shape and helmet fit matters in helmet safety: the contact area between a headform and helmet interior has been identified as a critical determinant of protection afforded by a helmet. The objective of this study was to compare quantitative measures of helmet fit between an adult male sample and the three 50<sup>th</sup> percentile male headforms (HFs). The following study recruited 42 adult male participants who wore a medium sized ice hockey helmet in an attempt to compare their quantitative helmet fit to those of three 50<sup>th</sup> percentile adult male HFs. Through 3D modeling, fit was quantified by assessing dimensional differences in two transverse cross-sectional planes of the head, and by using Principal Component Analysis (PCA) to determine the largest components of fit. Significant differences were found between the HFs and the participant's heads in anthropometrics and dimensional differences. The HFs were smaller than the participants' heads, demonstrating average gapping with the interior of the helmet. The principal components of fit extracted included medial-lateral warping, gapping/compression at the rear aspect of the helmet-head interface, and general congruence of the head shape to the helmet liner. These findings demonstrated incongruence in helmet fit between surrogate headforms and ordinary users.

#### 3.2 Introduction

Ice hockey is a popular recreational and competitive winter sport; however, the high incidence of sport related concussions is of concern [1]. For instance, in Canadian minor hockey, concussion is the most common specific injury type [2]. At the collegiate level, concussion is the most common injury in women's ice hockey, and second most common for men [3,4]. Ice hockey helmets were adopted as required equipment in competitive play in the 1980's to reduce the prevalence of head injuries, particularly skull fractures [5]. In order for ice hockey helmet models to be certified for commercial sale, sample helmets must pass a standardized series of controlled impact drop tests of helmet mounted on surrogate headforms [6–8].

According to most international testing standards, for medium sized ice hockey helmets, impact tests are performed on 50th percentile adult male surrogate headforms (circumference of 575mm about the Reference Plane) [8,62]. Peak linear acceleration has been the most common measurement criterion to be assessed for impact protection in the sports industry. The established pass/fail criterion for helmets standards are between 250-300g, believed to be the threshold for skull fracture; however, the extent to which certified helmets can reduce the incidence of concussion has been limited [9]. Notably, recent research has implicated high rotational accelerations as an important concussion risk factor [10,11], though to date no current hockey helmet standard includes rotational acceleration due to the complexity in defining repeatable testing methodology and criterion thresholds [9].

In addition to the above, on an elementary level, all standards state proper helmet fit is essential for helmet function; yet, other than a defined area of coverage and retention stability, a quantitative definition of helmet-to-head fit is lacking. However, recent evidence suggests that helmet-to-head size differences affect impact behaviour. In a study on motorcycle helmets, peak acceleration and Head Injury Criterion were measured using finite element modeling under two

conditions: first, different combinations of an allometrically scaled Hybrid III 50<sup>th</sup> percentile headform (at 0.8, 0.9, and 1.1 scale) with the original helmet; and second, the baseline Hybrid III headform with the allometrically scaled helmet (at 1.1 and 1.2 scale) [12]. These scaling factors, typically within a given helmet-to-head size pairing, substantially altered head impact responses. The authors stated that contact area between the interface of the headform and helmet liner was a critical determinant of protection afforded by the helmet to the headform. By extension, variations in the user's head shape proportions may further alter helmet fit and its protective capacity.

Similarly, surrogate head shape proportions may matter in terms of standardized testing protocols. For instance, different surrogate headform shapes used by NOCSAE, ASTM, ISO/CEN and CSA vary substantially on visual inspection. Further, the Hybrid III headform, developed within the automotive industry for crash test dummies, varies distinctively in shape and size from these other headforms [8,13]. The Hybrid III headform and neck combinations have been adopted by various research groups, given the multi-triaxial accelerometer configuration offers angular acceleration estimates. However, the Hybrid III headform was designed solely on the average cranial measurements of a collection of 16 Caucasian male adult skulls [14]. Likewise, the NOCSAE headform was designed based on average anthropometrics of 13 cadaver heads within the size range of the most popular football helmet size [15]. Between these two headforms substantial differences were noted in the back cranial regions [13].

The use of anthropometric averages to generalize a population should be done with caution. For example, the classic study examining the average of ten physical dimensions of over 4000 pilots revealed no single subject fell within the average range of all measured dimensions [16]. Thus, designing for an "average individual" risks being unsatisfactory for all users [16].

This fallacy is highlighted by a recent study, where differences in head shape were observed between a sample of adult males and standard headforms with the anthropometrics of a 50<sup>th</sup> percentile adult male [17]. For instance, a study of bicycle helmet fit demonstrated that female and Asian helmet users had lower fit scores than male and Caucasian users, respectively, for a given size of helmet [18]. Furthermore, using two large datasets of Caucasian and Chinese head shapes obtained by using 3D laser scanning technology, Ball et al. revealed significant variations in size, shape, and proportion between the two demographics [19].

Hence, the rationale for this study is to address a potential disconnect between standard headforms and actual users with regards to helmet fit. Using the protocol developed by Greencorn [20], this study will quantitatively compare helmet fit between headforms and a sample of adult males. We hypothesize differences will be observed in the way helmets fit on headforms and on humans, in terms of both the gapping and compression of the foam liner at the helmet-to-head interface. Further, it is expected distinct head-helmet fit profiles, in terms of regional locations of relative gapping and compression of the helmet liner, will be observed.

### 3.3 Methods

#### **3.3.1** Ethics

The methods involved in this research study have been approved by the McGill Human Research Ethics Board II criteria (certificate # 135-0816).

## 3.3.2 Participants

The subjects for this study were adult males (n=42). The inclusion criteria for the human subjects consisted of adult males between the ages of 18-60 and having played hockey regularly within three years of participation in this study.

In addition, the shapes of three standard headforms (fig. 1 a-c) used for impact testing (medium 50<sup>th</sup> percentile NOCSAE, Hybrid III, and CEN EN960, n=3) were collected. Each headform has a head circumference of 575-580 mm about the Reference Plane, defined by each standard at a certain height above the Frankfurt Plane (transverse plane passing through the inferior borders of the bony orbit and the upper margins of the auditory meatus). To enhance the quality of the rendered 3D model, the headforms were coated with a matte spray to reduce the reflectiveness of the headforms.







**Figure 1** The three medium headforms used in the study: a) NOCSAE; b) CEN EN960; c) Hybrid III.

#### **3.3.3** Helmet

3D models of the Bauer IMS 9.0 helmet (medium size) were reconstructed. Given this helmet model's ability for telescopic adjustment in front-to-back length, all seven available adjustment increments were scanned (that is, a range of interior circumference from 560-600mm and exterior circumference from 715-755mm). The new helmet was supplied by Bauer Hockey Ltd. Helmet logos were covered to blind the participant to the make and model of the helmet. Like the headforms, the helmet was coated with a matte spray to reduce the reflectiveness of the helmet shell.

## 3.3.4 Equipment and Software

Photogrammetry is a technique that constructs 3D models from overlapping digital images. Two Canon EOS Rebel T7i/800D cameras each with a Canon EF 40mm f/2.8 STM Lens (Canon Canada Inc., Mississauga, Ontario, 2015) were used to take synchronized photos (6000x4000 pixel resolution). These captured, first, the concave shape of the helmet interior and, second, the exterior cranial head shape of subjects. The two cameras were mounted at different camera heights on a tripod, each angled to centre the helmet or subject in the frame. A remote shutter was connected to the two cameras via a jack splitter, allowing for the simultaneous capture of two levels and angles of the desired object. Using the remote shutter eliminated potential movement of the camera introduced when pressing the shutter button to take photos.

AutoDesk® ReCap™ (Autodesk Inc., 2017) was used to render each series of digital photos into scaled 3D models; 3D Builder © (Microsoft Corp., Redmond, Washington, USA, 2015) was used to process the 3D models; and MeshLab (open source program, 2016) was used to align the helmets to the heads. MATLAB® (MathWorks Inc. Natick, Massachusetts, USA, 2016) and SPSS® (IBM Corp., Armonk, New York, USA, Version 23.0, 2015) were used for data analysis.

### 3.3.5 Protocol

Following the recommendations made by Greencorn [20], the protocol was modified to include improvements to the photogrammetry protocol. 3D models of the subjects and helmets were created using the two camera setup. A series of photos were taken simultaneously at two different camera heights and angles to capture the entire surface of the desired object. These photos were then rendered into scaled 3D models using the software Autodesk® ReCap<sup>TM</sup>.

## 3.3.6 Participant Testing Protocol

For the adult subjects, participants wore a clean spandex cap to reduce hair artifacts and a compression shirt to minimize shirt movement between photos. Each participant sat on a chair (HermanMiller Caper Multipurpose Stool) permitting transverse rotation. The photo-capture setup (fig. 2) involved two cameras both mounted on one tripod stationed 1m front of the chair, flanked by two illuminated softboxes (Westcott Basics uLite Tungsten 500W), with a uniform textile backdrop suspended behind the chair.

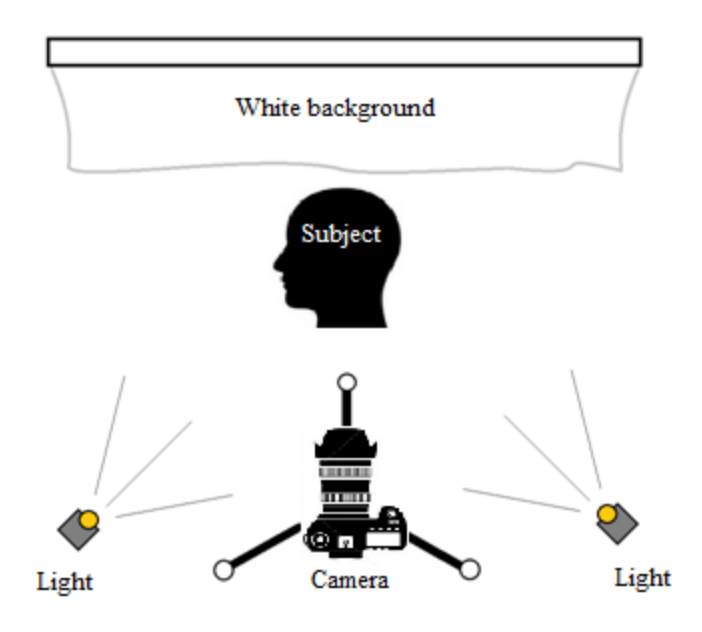


Figure 2 Photo-capture setup. Two cameras at different heights were used.

### 3.3.6.1 Anthropometric Measurements

All anthropometric measurements were taken by the same investigator, using a 30cm caliper (Lafayette Instrument Company, model 01291, 1mm increments with 0.5mm accuracy). Anterior-posterior measurements were taken at 25mm above the eyebrow line along the median plain to the apex of the occipital bone. Medial-lateral measurement was taken from just above the peak of both ears. Similar anterior-posterior and medial-lateral measurements were taken when the subject was wearing the helmet. The magnitude of medial-lateral and anterior-posterior helmet warping were determined by taking the difference between these measures when the helmet was not being worn and when it was on the subject's head. Circumference was taken with a tape measure going through these reference points.

To account for the compressibility of superficial tissues possible with the adult subject heads, but absent from the headforms, compressed length and width measurements were taken at the same anterior-posterior and medial-lateral head locations. This was achieved by using the same calipers to apply compression, to the level indicated by subjects that they perceived as matching the typical compression applied by a helmet.

#### **3.3.6.2 Head Scan**

The cameras were oriented in portrait to maximize the image space occupied by the subject. Each camera was positioned at a different height on the tripod (i.e. aligned to the mid horizontal level of the head and 0.3m above). Participants were asked to maintain neutral head position and facial expression with eyes closed. Following each camera shutter sound, participants were instructed to rotate the seat of the chair with their feet ( $\sim$ 7°) in a clockwise direction. Photos were taken for one complete revolution of the subject, for a total of approximately 100 photos per subject. Each complete revolution was photographed at two

different camera heights, with the pitch of the cameras adjusted to keep the helmet/subject centered. This was repeated with the subject wearing the hockey helmet, producing a helmet/head scan hereafter referred to as the intermediate scan. This is an amendment from Greencorn [20]; in the previous protocol, 3D scans were created from still frames exported from high-definition (1920×1080 px) video of the revolving subject, rather than from high resolution still photographs (6000 x 4000 px). The revised method produced higher resolution intermediate models than those used in Greencorn [20] for two reasons: first, the increased resolution of the images used for photogrammetry, and second, minimized motion artifact introduced by the participant rotating in the videos.

A similar photo capture setup was used for the headforms, with the headform sitting on a turntable placed on a table. The turntable was rotated manually at increments of approximately 7°, for one complete revolution with the two cameras capturing two different perspectives of the headform. Following the collection of the photos, each series of digital images were inputted into AutoDesk® ReCap<sup>TM</sup> to render a high-definition scaled 3D model of the subject. These models consisted of up to 10 vertices per square millimeter, for a minimum of 500,000 vertices per subject model.

Following image collection, a series of data processing steps were required to calculate dimensional differences (DD), defined as the differences between the radial distances of the helmet's interior liner and the head's surface. Specifically, DD are the difference between each corresponding rho value of the 360 polar coordinates of the head and the helmet. Figure 3 depicts the protocol of the current study.

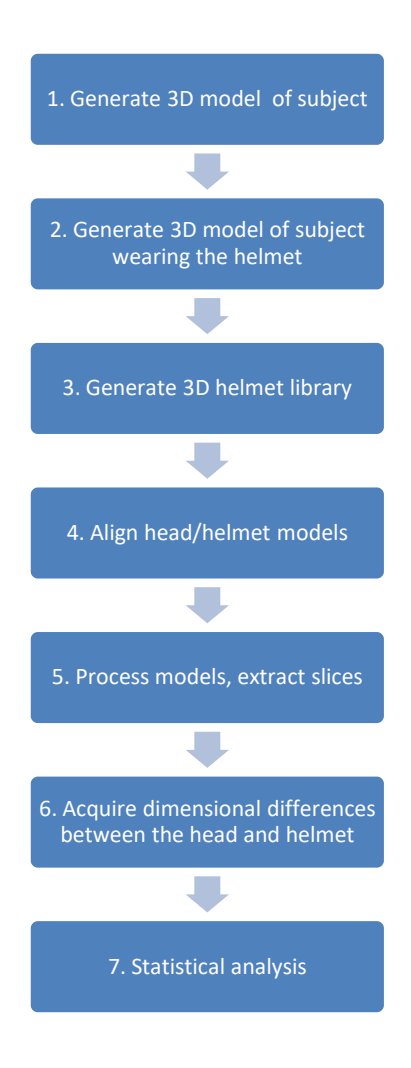


Figure 3 Study Protocol. Step 1 described above; steps 2-7 detailed below.

## 3.3.7 Helmet on Head (Intermediate) Scans

The adult subjects were the helmet at their preferred size and adjustment setting. For the surrogate headforms, helmets were mounted onto the headforms based on the same criteria used for helmet impact testing: medium sized helmet on a 50<sup>th</sup> percentile headform, helmet set to the tightest allowable adjustment, front edge of the helmet aligned to a pre-marked line on the forehead of the headform, and helmet centered by eye.

#### 3.3.8 Create 3D Helmet Models

Using the photo-capture setup (fig. 2) and following the protocol used with the headforms, approximately 100 photos were taken of the exterior and interior surfaces of the helmet model at each adjustment setting. These photos were the imported into AutoDesk® ReCap<sup>TM</sup> and subsequently rendered into a 3D model.

## 3.3.9 Data Processing

The data processing followed the same procedure used in Greencorn [20]. This involved trimming, scaling, and exporting the 3D models, aligning the 3D models, and calculating DD.

All 3D models were scaled using a ruler or caliper in the model as the reference.

## 3.3.9.1 3D Model Preparation

All 3D models were scaled and trimmed to contain only the objects of interest (i.e. head, helmet, helmet on head) in AutoDesk® ReCap<sup>TM</sup>. Subsequently, these were exported as "\*.ply" (Polygon File Format, hereby referred to as a "point cloud"). In 3D Builder©, the head point clouds were coloured black, and the helmet point clouds were coloured white. This step was performed to facilitate data processing; as point cloud data also contains colour specification, points of the head and the helmet were differentiated by colour.

## 3.3.9.2 Scan Alignment

Alignment of the helmet onto the head was necessary to measure the DD. The coloured point clouds were imported into MeshLab to be aligned. The alignment tool "Point Based Gluing" uses an iterative closest point algorithm to reduce the distances between selected landmarks on the two point clouds to be aligned. Using this tool, facial landmarks were selected to best orient a subject's head point cloud on their intermediate point cloud. The corresponding helmet point cloud, at the size and adjustment used by the subject, was aligned using the same

tool to the helmet portion of the intermediate point cloud. Once the alignments of the helmet and head point clouds were completed, the intermediate point cloud was removed; the helmet and head point clouds were then merged and exported as a single aligned point cloud, with the head coloured black, and the helmet coloured white.

The resulting aligned point clouds were oriented in 3D Builder  $\mathbb{C}$  to position the helmet referenced plane (fig. 4a-c) at the (0, 0) x, y plane. This plane will hereafter be referred to as the "Helmet Plane".



Figure 4a Helmet Plane from rear view; landmarks: bottom ridge of rear boss vent.



Figure 4b Helmet Plane from front view; landmark: middle of front groove.

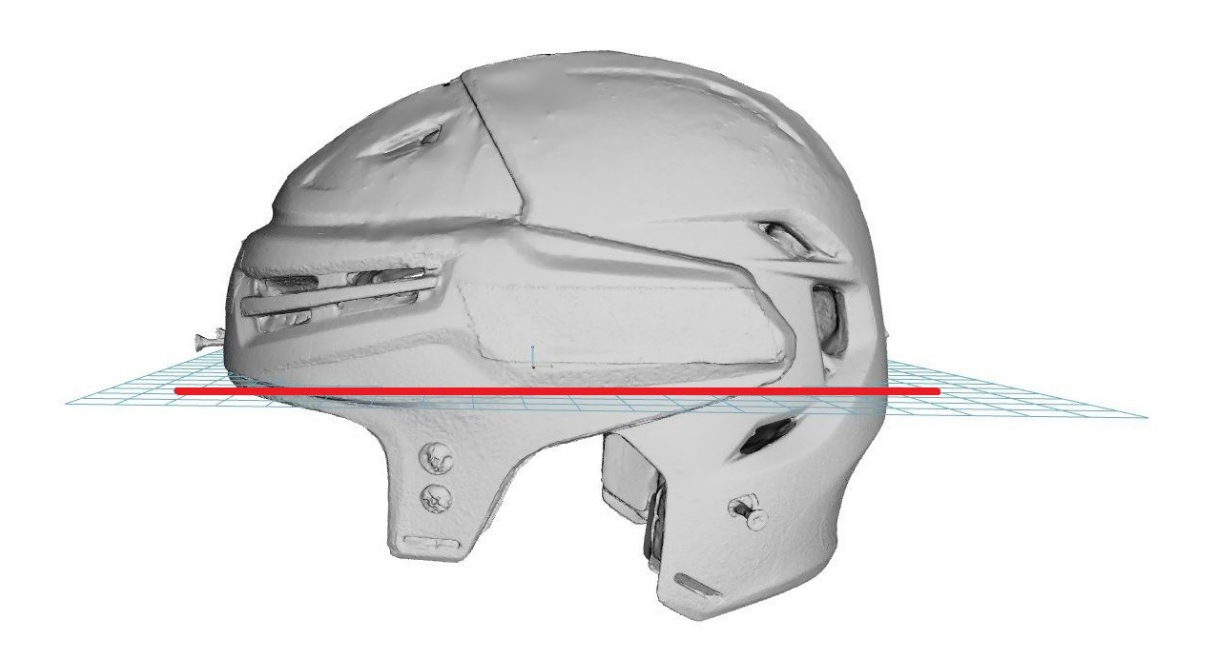


Figure 4c Helmet Plane side view.

## 3.3.9.3 Alignment Error

Root mean square error (RMSE) was used to estimate the error in the alignment of the high resolution head and helmet models to the high resolution intermediate model. One high resolution head model and one high resolution helmet model were aligned five times using the same high resolution intermediate model. The DD values for each alignment were determined, then RMSE values were determined between pairs of alignments for all possible combinations of pairs. These were then averaged for an RMSE value of 0.40mm. This is an improvement from Greencorn [20], where RMSE for alignment was 1.14mm.

## 3.3.9.4 Measuring Dimensional Differences

From the aligned 3D models, two 2D "slices" parallel to the Helmet Plane were analyzed.

Custom MATLAB scripts were developed in Greencorn [20] to slice the aligned helmet and head models at any distance above or below the Helmet Plane and output DD between the head and

the helmet. DD measured from slices at 0 and 20mm (i.e. Plane 1 and Plane 2, respectively) above the Helmet Plane were used for analysis.

## 3.3.10 Statistical Analysis

All statistical analyses were completed using SPSS Statistics software (IBM Corporations, Somers, U.S.A., Version 23.0) and MATLAB® (MathWorks Inc. Natick, Massachusetts, USA, 2016). The mean, maximum, minimum, and standard deviations of anthropometric measures were calculated. One sample t-tests were used to compare the mean of adult subjects to each of the headforms in circumference, length, compressed length, width, compressed width, length-to-width ratio, compressed length-to-compressed width ratio, and DD values.

An additional sub-analysis was completed with subjects wearing the same helmet adjustment as the headforms. One sample t-tests were performed on the mean of this subsample to each of the headforms in the same anthropometric measures. Paired sample t-tests were used to compare length, width, and length-to-width ratio measurements to compressed length, compressed width, and compressed length-to-compressed width ratio, respectively. To compare the different aspects of helmet fit, Principal Component Analysis was run for the DD of the adult subject heads and for the headforms. The PC scores of the three headforms were calculated by projecting their waveform data with the group mean of the adult subjects removed onto each PC [63]. Lastly, Pearson product-moment correlation coefficients for PC scores and head anthropometrics were calculated to identify relations between head anthropometrics and principal components.

#### 3.4 Results

The following results describe the range of human subjects' heads (HS) and headform (HF) anthropometrics recorded. Subsequently, the Principal Component Analysis findings of DD head-helmet fit at Plane 1 and Plane 2 will be presented.

## 3.4.1 Head Shape and Headform Anthropometrics

Anthropometrics of the HS and the medium sized surrogate HFs are presented in Table 1. The average head dimensions of the subjects in this study were larger than those found in anthropometric databases (length:  $195 \pm 8$ mm; width:  $155 \pm 6$ mm) [54]. Given that subjects of the study were medium sized helmets, thus including only participants in the median range, these differences were unexpected. Furthermore, significant differences were observed between the mean of the HS and each of the HFs across all standard anthropometric measures (i.e. circumference, length, and width) and other measures (Table 2a-c).

The length and width measurements of the HS were both significantly greater than their respective compressed measurement (length: t=14.108, p<0.001; width: t=21.918, p<001). Furthermore, the length measurements of each HF were significantly less than the mean compressed length of the HS. With mean compressed width of the HS, the width of the NOCSAE HF was observed to be significantly less (t=2.772, p<0.01).

Length-to-width (L:W) ratios of the HS ranged from 1.2 to 1.4, while the compressed length to compressed width (cL:cW) ratios ranged from 1.19 to 1.44. The L:W ratio of the HS were significantly less than their respective cL:cW ratio (t=13.787, p<0.001). The NOCSAE HF was significantly greater in L:W ratio from the sample mean (t=-2.671, p<0.05). With regards to the ratio of compressed length to compressed width, both the Hybrid III (t=3.085, p<0.005) and the CEN EN960 (t=4.221, p<0.001) HFs were significantly smaller than the ratio of the HS.

With regards to the magnitude of helmet warping, the NOCSAE HF and mean of the HS were similar in both directions (anterior-posterior: t=1.058, p>0.05; medial-lateral: t=1.307, p>0.05). However, the Hybrid III HF was observed to be significantly greater in the magnitude of anterior-posterior warping (t=-5.00, p<0.001), but not significantly different in the magnitude of medial-lateral warping (t=1.307, p>0.05). The CEN EN960 HF dempostrated significantly less helmet warping in both directions when compared with the HS (anterior-posterior: t=5.095, p<0.001; medial-lateral: t=4.053, p<0.001).

**Table 1** Anthropometrics of the HS and the three different HFs (units in mm).

|   | HS           | NOCSAE | Hybrid III | CEN EN960 |
|---|--------------|--------|------------|-----------|
| Mean circumference (standard deviation) | 587.7 (12.0) | 575    | 580        | 575       |
| Circumference minimum, maximum          | 559, 612     |        |            |           |
| Mean length (standard deviation)        | 207.2 (5.3)  | 200    | 201        | 199       |
| Mean compressed length (standard        |              |        |            |           |
| deviation)                              | 204.2 (5.8)  | 200    | 201        | 199       |
| Length minimum, maximum                 | 194.5, 221   |        |            |           |
| Compressed length minimum, maximum      | 190, 219     |        |            |           |
| Mean value of AP compression (standard  |              |        |            |           |
| deviation)                              | 3.0 (1.37)   | n/a    | n/a        | n/a       |
| Mean width (standard deviation)         | 161.0 (5.4)  | 153    | 156        | 155       |
| Mean compressed width (standard         |              |        |            |           |
| deviation)                              | 155.2 (5.1)  | 153    | 156        | 155       |
| Width minimum, maximum                  | 150, 171.5   |        |            |           |
| Compressed width minimum, maximum       | 145, 165.5   |        |            |           |
| Mean value of ML compression (standard  |              |        |            |           |
| deviation)                              | 5.8 (1.72)   | n/a    | n/a        | n/a       |
| Mean L:W ratio (standard deviation)     | 1.29 (0.05)  | 1.31   | 1.29       | 1.28      |
| Mean cL:cW ratio (standard deviation)   | 1.32 (0.06)  | 1.31   | 1.29       | 1.28      |
| L:W ratio minimum, maximum              | 1.18, 1.40   |        |            |           |
| cL:cW ratio minimum, maximum            | 1.19, 1.44   |        |            |           |
| Mean helmet AP warping (standard        |              |        |            |           |
| deviation)                              | 2.3 (1.6)    | 2.0    | 3.5        | 1.0       |
| AP helmet warping minimum, maximum      | 0, 7.0       |        |            |           |
| Mean helmet ML warping (standard        |              |        |            |           |
| deviation)                              | 0.7 (1.2)    | 0.5    | 0.5        | 0         |
| ML helmet warping minimum, maximum      | -1.5, 3.0    |        |            |           |

**Table 2** One sample t-test of HS measurements, using HF measurements as the test value (estimated population mean): a) NOCSAE; b) Hybrid III; c) CEN EN 960. Significant differences are denoted with asterisks.

a)

|                        | Circumference | Length  | Compressed  | Width   | Compressed | L:W    | cL:cW  | AP     | ML     |
|------------------------|---------------|---------|-------------|---------|------------|--------|--------|--------|--------|
|                        | (mm)          | (mm)    | length (mm) | (mm)    | width (mm) | ratio  | ratio  | warp   | warp   |
|                        |               |         |             |         |            |        |        | (mm)   | (mm)   |
| Mean of HS             | 587.7         | 207.2   | 204.2       | 161.0   | 155.2      | 1.29   | 1.32   | 2.3    | 0.7    |
| Standard deviation     | 12.0          | 5.3     | 5.8         | 5.3     | 5.1        | 0.05   | 0.06   | 1.6    | 1.2    |
| NOCSAE<br>(test value) | 575*          | 200*    | 200*        | 153*    | 153*       | 1.31*  | 1.31   | 2.0    | 0.5    |
| t-statistic            | 6.863         | 8.842   | 4.68        | 9.682   | 2.77       | -2.671 | 0.812  | 1.058  | 1.307  |
| Significance           | p<0.001       | p<0.001 | p<0.001     | p<0.001 | p<0.01     | p<0.05 | p>0.05 | p>0.05 | p>0.05 |
| df                     | 41            | 41      | 41          | 41      | 41         | 41     | 41     | 41     | 41     |

b)

| ~,           |               |         |             |         |            |        |         | _       |        |
|--------------|---------------|---------|-------------|---------|------------|--------|---------|---------|--------|
|              | Circumference | Length  | Compressed  | Width   | Compressed | L:W    | cL:cW   | AP      | ML     |
|              | (mm)          | (mm)    | length (mm) | (mm)    | width (mm) | ratio  | ratio   | warp    | warp   |
|              |               |         |             |         |            |        |         | (mm)    | (mm)   |
| Mean of HS   | 587.7         | 207.2   | 204.2       | 161     | 155.2      | 1.29   | 1.32    | 2.3     | 0.7    |
| Standard     | 12.0          | 5.3     | 5.8         | 5.4     | 5.1        | 0.05   | 0.1     | 1.6     | 1.2    |
| deviation    |               |         |             |         |            |        |         |         |        |
| Hybrid III   | 580*          | 201*    | 201*        | 156*    | 156        | 1.29   | 1.29*   | 3.5*    | 0.5    |
| (test value) |               |         |             |         |            |        |         |         |        |
| t-statistic  | 4.156         | 7.601   | 3.56        | 6.046   | -1.05      | -0.221 | 3.085   | -5.00   | 1.307  |
| Significance | p<0.001       | p<0.001 | p=0.001     | p<0.001 | p>0.05     | p>0.05 | p<0.005 | p<0.001 | p>0.05 |
| df           | 41            | 41      | 41          | 41      | 41         | 41     | 41      | 41      | 41     |

c)

|              | Circumference | Length | Compres | Width | Compressed | L:W    | cL:cW   | AP warp | ML warp |
|--------------|---------------|--------|---------|-------|------------|--------|---------|---------|---------|
|              | (mm)          | (mm)   | sed     | (mm)  | width (mm) | ratio  | ratio   | (mm)    | (mm)    |
|              |               |        | (mm)    |       |            |        |         |         |         |
|              |               |        | length  |       |            |        |         |         |         |
| Mean of HS   | 587.7         | 207.2  | 204.2   | 161.0 | 155.2      | 1.29   | 1.32    | 2.3     | 0.7     |
| Standard     | 12.0          | 5.3    | 5.8     | 5.4   | 5.1        | 0.1    | 0.1     | 1.6     | 1.2     |
| deviation    |               |        |         |       |            |        |         |         |         |
| CEN EN960    | 575*          | 199*   | 199*    | 155*  | 155        | 1.28   | 1.28*   | 1.0*    | 0*      |
| (test value) |               |        |         |       |            |        |         |         |         |
| t-statistic  | 6.775         | 10.075 | 5.80    | 7.258 | 0.23       | 1.003  | 4.221   | 5.095   | 4.053   |
| Significance | p<0.001       | p<0.00 | p<0.001 | p<0.0 | p>0.05     | p>0.05 | P<0.001 | p<0.001 | P<0.001 |
|              |               | 1      |         | 01    |            |        |         |         |         |
| df           | 41            | 41     | 41      | 41    | 41         | 41     | 41      | 41      | 41      |

### 3.4.2 Helmet Dimensional Differences

The mean values of dimensional difference (DD) between helmet and head are listed in Table 3. For Slice 1 and Slice 2, the mean DD values for each HF were determined, in addition to the mean, standard deviation, minimum, and maximum of the averaged DD values of the HS. At Slice 1, the average DD value for the HS was negative (-2.17mm  $\pm$  1.40 SD), indicating average compression at the head-helmet interface. Each of the three HFs had positive average DD values, indicating gapping at the head-helmet interface (fig. 5a). The mean DD of the HFs were each significantly greater than the HS (p<0.001). At Slice 2, the average DD value for the HS was positive (0.31mm  $\pm$  1.53 SD), indicating average gapping at the head-helmet interface. The average DD values of each of the HFs were also positive and greater in magnitude than the average of the HS (fig. 5b). The average DD of the HFs were significantly greater than HS (p<0.001).

**Table 3** Mean DD values at Slice 1 and Slice 2 (units in mm). Significant differences are denoted with asterisks.

|                        | HS           | NOCSAE      | Hybrid III           | CEN EN960            |
|------------------------|--------------|-------------|----------------------|----------------------|
| Slice 1 Mean DD (± SD) | -2.17 (1.40) | 1.19*       | 0.58*                | 0.08*                |
|                        |              | (t=-15.612, | ( <i>t</i> =-12.778, | ( <i>t</i> =-10.456, |
|                        |              | p<0.001)    | p<0.001)             | p<0.001)             |
| Slice 1 DD minimum,    | -4.69, 0.96  |             |                      |                      |
| maximum                |              |             |                      |                      |
| Slice 2 Mean DD        | 0.31 (1.53)  | 2.38*       | 1.39*                | 1.80*                |
| (standard deviation)   |              | (t=-8.795,  | (t=-4.590,           | ( <i>t</i> =-6.332,  |
|                        |              | p<0.001)    | p<0.001)             | p<0.001)             |
| Slice 2 DD minimum,    | -2.87, 3.80  |             |                      |                      |
| maximum                |              |             |                      |                      |

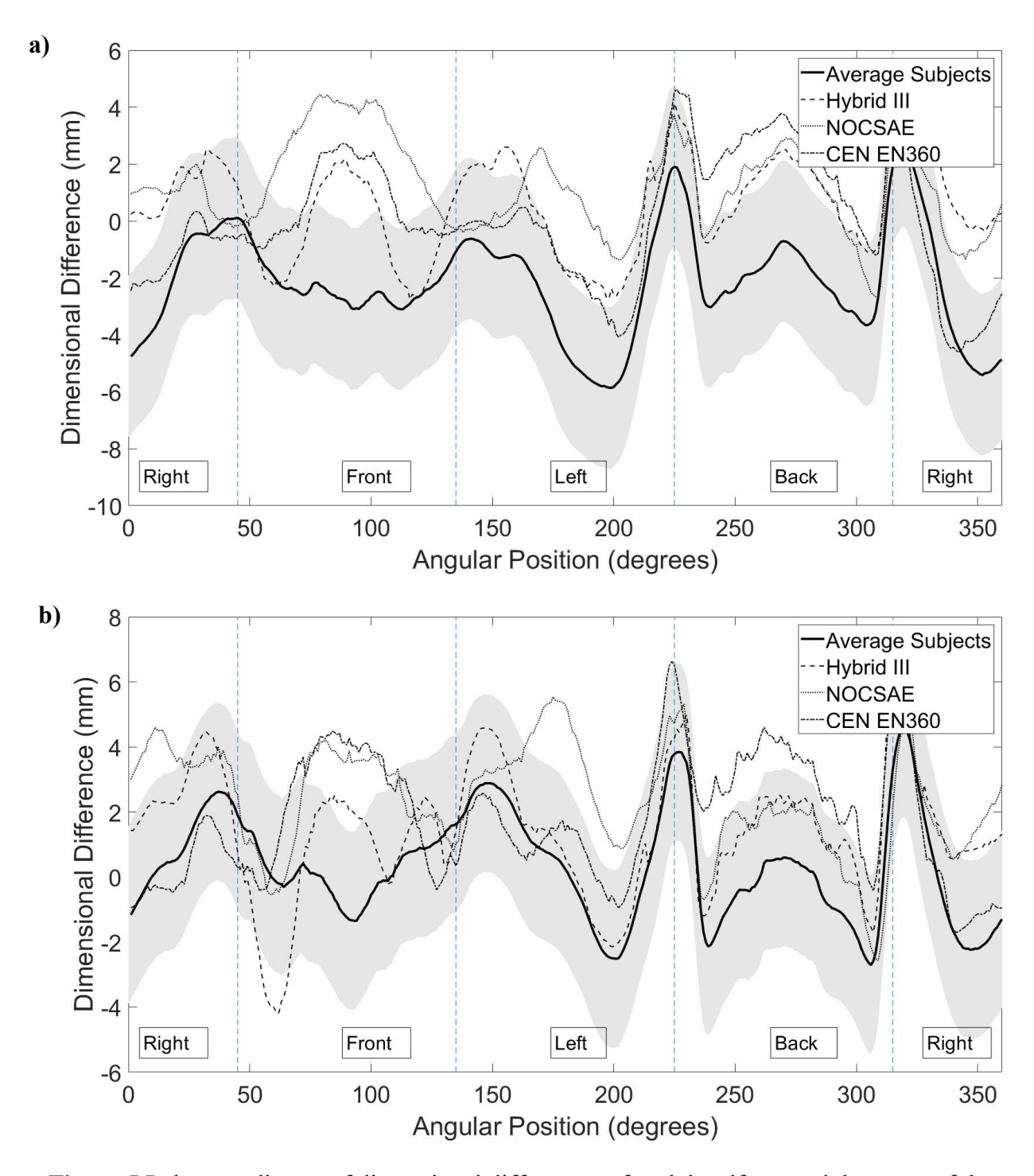


**Figure 5** Polar coordinates of dimensional differences of each headform and the mean of the subjects, with standard deviation of the HS in grey: a) Slice 1; b) Slice 2.

# 3.4.3 Principal Component Analysis of Dimensional Differences

Principal component analysis (PCA) was used to analyze DD waveforms for each helmet and head/headform combination at Slice 1 (fig. 6 and 7) and Slice 2 (fig. 8 and 9). The figures below depict the eigenvector (i.e. principal component or PC), the position and magnitude of the variance in the eigenvalues or variance of the data (denoted as the grey shaded area in fig. 6-9 (a)), high and low scores for each of the PCs (5 participants averaged inside each of the 5<sup>th</sup> and 95<sup>th</sup> percentiles) (fig. 6-9 (b)), and the Cartesian representation of the 5<sup>th</sup> (fig. 6-9 (c)) and 95<sup>th</sup> (fig. 6-9 (d)) percentile helmet-head combinations. High and low PC scores represent the extreme ends of the feature of variance described by the PC. For example, if a PC represents head width, a high score would indicate greater width and a low score would show a narrow HS. The high and low traces depict the average of five high scoring subjects and five low scoring subjects, respectively; an average was used to offset the influence of possible outliers on the shape of the trace. Two PCs were extracted from Slice 1 and Slice 2, cumulatively accounting for 66% and 61% of the variation of the DD waveforms, respectively. For each PC, PC scores were determined for the HFs; the corresponding ranks of each HF's PC score (Table 4), relative to the PC scores of the HS (n=42), are listed with each PC interpretation.

Table 5 represents correlation coefficients determined for PC scores and head anthropometric measurements. Corresponding PC waveform and anthropometric correlation measures were used to interpret the helmet-to-head fit properties explained by each principal component.

Slice 1 PC1 (fig. 6) represents 40.0% of the variance in the DD waveform, and corresponds with the medial-lateral warping of the helmet. PC score and head anthropometric correlations with significance were circumference (r= -0.393, p<0.05), width (r= -0.847, p<0.001), L:W ratio (r= 0.780, p<0.001), cL:cW ratio (r=0.756, p<0.001) and magnitude of

helmet warping in the medial-lateral direction (r= -0.463, p<0.005). The high PC1 scores correspond to less compression and greater gapping at the lateral aspects of the helmet. As well, these waveforms are correlated with narrow HS and less warping of the helmet in the medial-lateral direction. Additionally, the five HS waveforms comprising the high PC trace of PC1 fall within the narrowest width measurements. Low PC scores for PC1 show greater compression at the lateral aspects of the head; these waveforms are also correlated with larger, rounder HS. The PC1 scores of the NOCSAE, Hybrid III, and CEN EN960 HFs are ranked 35<sup>th</sup> (83%ile), 34<sup>th</sup> (81%ile), and 22<sup>nd</sup> (52%ile), respectively

Slice 1 PC2 (fig. 7) represents 25.7% of the variance in the DD waveform, representing gapping/compression at the rear aspect of the head-helmet interface, with PC2 scores correlated with magnitude of helmet warping in the anterior-posterior direction (r= -0.460, p<0.005). High PC2 scores show gapping, and thus, looser fit, relative to the selected helmet adjustment. Low PC scores of PC2 show greater compression at the front and back regions of the head, displaying tighter fit relative to the selected helmet adjustment. The PC scores of PC2 of the NOCSAE, Hybrid III, and CEN EN960 HFs are ranked  $42^{nd}$  (100%ile),  $41^{st}$  (98%ile), and  $42^{nd}$  (100%ile), respectively.

The second plane analyzed of the head-to-helmet interface (Slice 2) is 20 mm higher than Slice 1. Slice 2 PC1 (fig. 8) represents 32.6% of the variance in the DD waveform, and corresponds with congruence between head shape and helmet liner. PC1 scores are correlated with width (r=0.4971, p<0.001), L:W ratio (r=-0.403, p<0.01), cL:cW ratio (r=-0.393, p<0.01), and magnitude of helmet warping in the anterior-posterior direction (r=-0.446, p<0.005). High PC1 scores show wider, rounder HS with greater overall congruence to the helmet liner, despite gapping at the rear aspect of the helmet-head interface. Low scores of PC1 show narrower, more

oblong HS with less congruence to the helmet liner, demonstrating both compression at the rear and gapping at the front bosses of the head-helmet interface. The PC scores of the NOCSAE, Hybrid III, and CEN EN960 HFs for PC1 are ranked 24<sup>th</sup> (57%ile), 29<sup>th</sup> (69%ile), and 37<sup>th</sup> (88%ile), respectively.

Slice 2 PC2 (fig. 9) represents 28.9% of variance in the DD waveform, and corresponds with the medial-lateral warping of the helmet. PC score and head anthropometric correlations demonstrating significance are width (r=0.5785, p<0.001), L:W ratio (r= 0.560, p<0.001), cL:cW ratio (r= 0.545, p<0.005), and magnitude of helmet warping in the medial-lateral direction (r= -0.362, p<0.05). High PC2 scores show less medial-lateral warping of the helmet, as these HS are more oblong in shape. Low PC2 scores show greater medial-lateral buckling of the helmet, as these HS are shorter and wider (i.e. rounder). For PC2, the PC score ranks of the NOCSAE, Hybrid III, and CEN EN960 HFs are  $39^{th}$  (93%ile),  $29^{th}$  (69%ile), and  $30^{th}$  (71%ile), respectively.

**Table 4** Ranks of the headform PC scores relative to the 42 HS; low scores were ranked between 1 and 14, median scores between 15 and 28, and high scores between 29 and 42. Percentile of PC score rank in brackets.

| Slice 1 | Headform   | PC1                    | PC2                     |
|---------|------------|------------------------|-------------------------|
|         | NOCSAE     | 35 (83 <sup>rd</sup> ) | 42 (100 <sup>th</sup> ) |
|         | Hybrid III | 34 (81 <sup>st</sup> ) | 41 (98 <sup>th</sup> )  |
|         | CEN EN960  | 22 (52 <sup>nd</sup> ) | 42 (100 <sup>th</sup> ) |
| Slice2  | NOCSAE     | 24 (57 <sup>th</sup> ) | 39 (93 <sup>rd</sup> )  |
|         | Hybrid III | 29 (69 <sup>th</sup> ) | 29 (69 <sup>th</sup> )  |
|         | CEN EN960  | 37 (88 <sup>th</sup> ) | 30 (71 <sup>st</sup> )  |

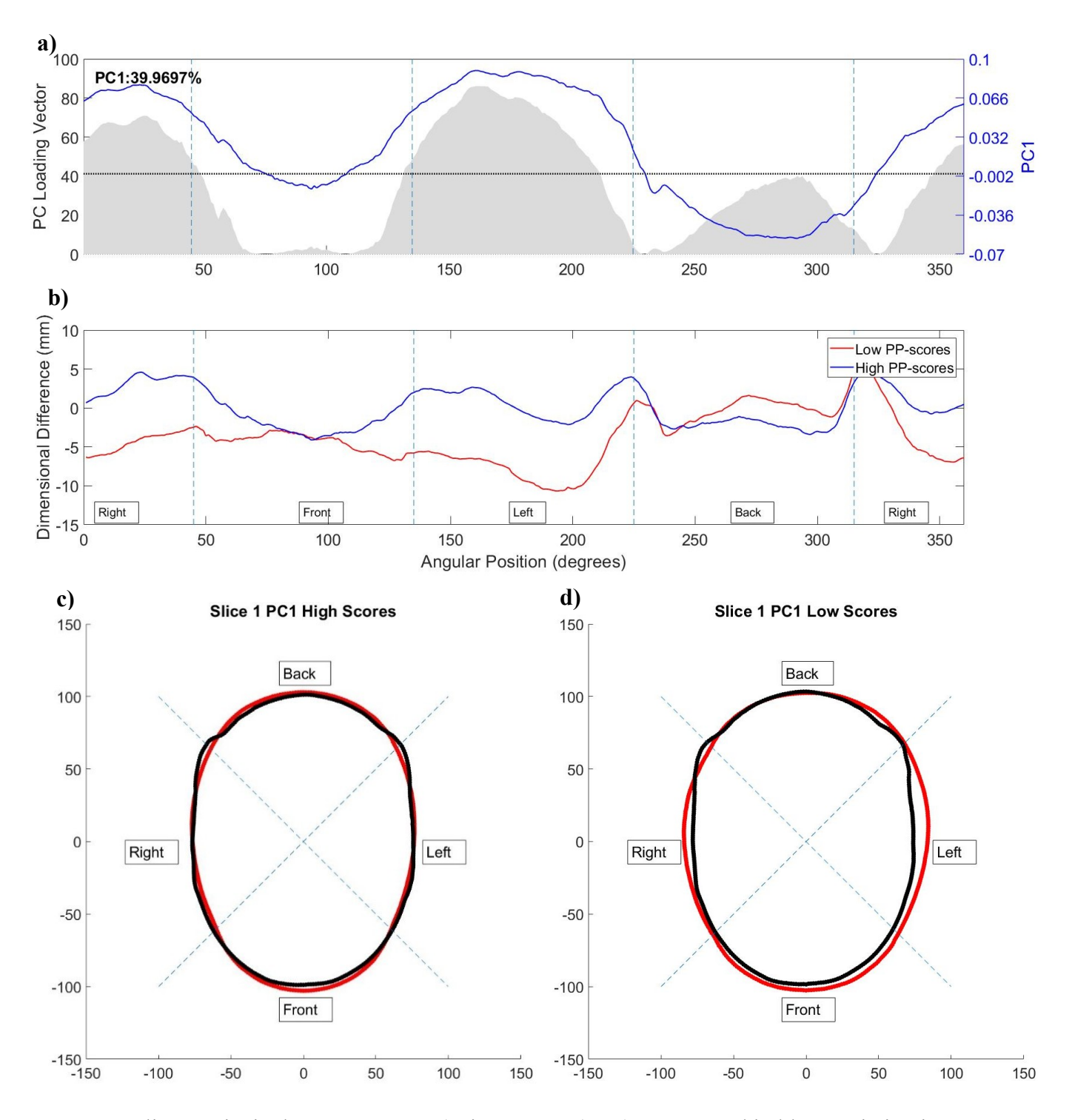


**Figure 6** Slice 1 Principal Component 1: a) eigenvector (PC1) represented in blue, variation in the principal component in grey; b) polar coordinate representations of 5<sup>th</sup> and 95<sup>th</sup> percentile PC1 scores; c) Cartesian representation of 95<sup>th</sup> percentile PC1 scores, red representing the outline of the head, black representing the outline of the helmet liner; d) Cartesian representation of 5<sup>th</sup> percentile PC1 scores, red representing the outline of the head, black representing the outline of the helmet liner.

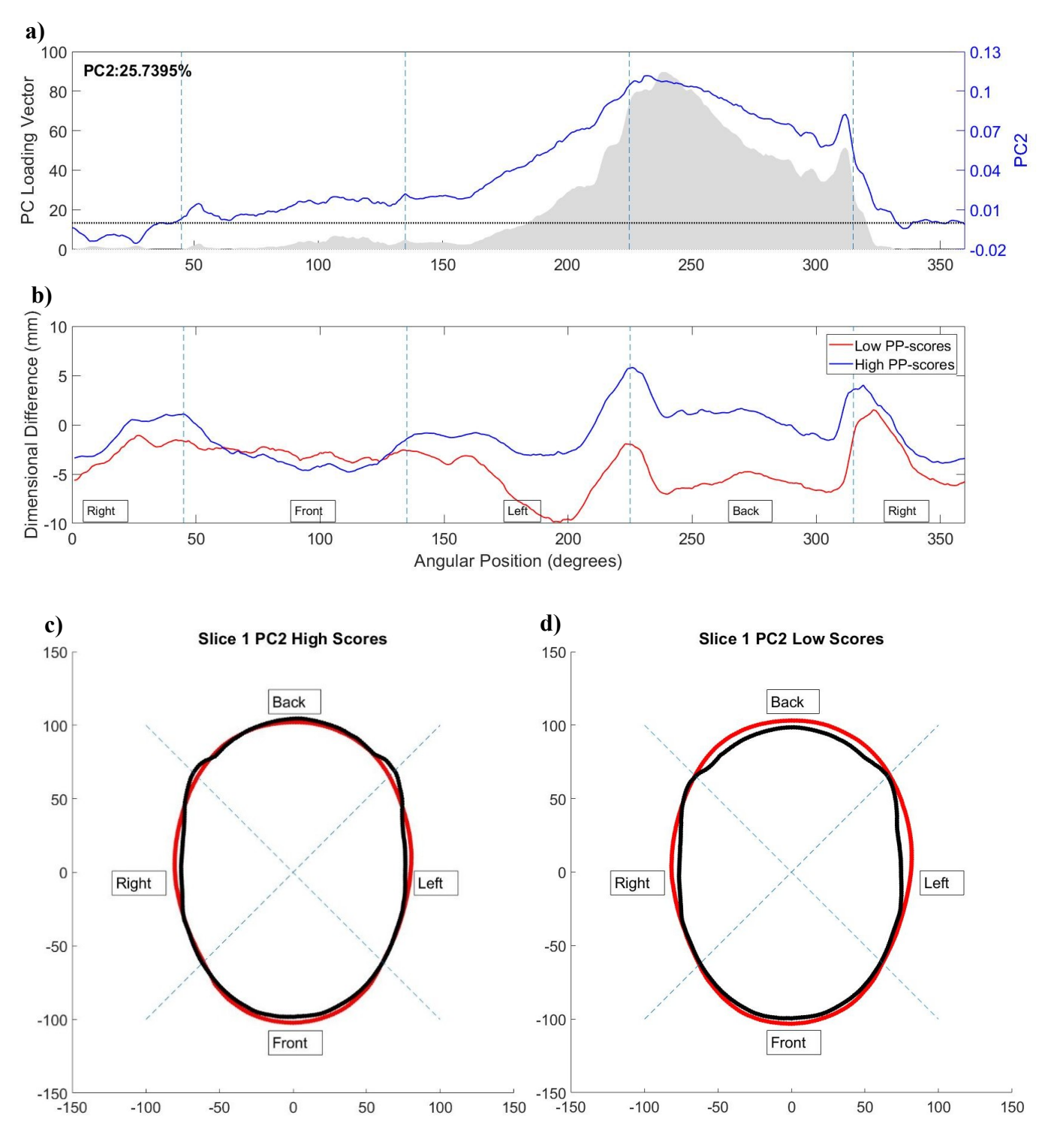


**Figure 7** Slice 1 Principal Component 2: a) eigenvector (PC2) represented in blue, variability in the principal component in grey; b) polar coordinate representations of 5<sup>th</sup> and 95<sup>th</sup> percentile PC2 scores; c) Cartesian representation of the 95<sup>th</sup> percentile PC2 score, red representing outline of head, black representing outline of helmet liner; d; Cartesian representation of 5<sup>th</sup> percentile PC2 score, red representing outline of head, black representing outline of helmet liner.

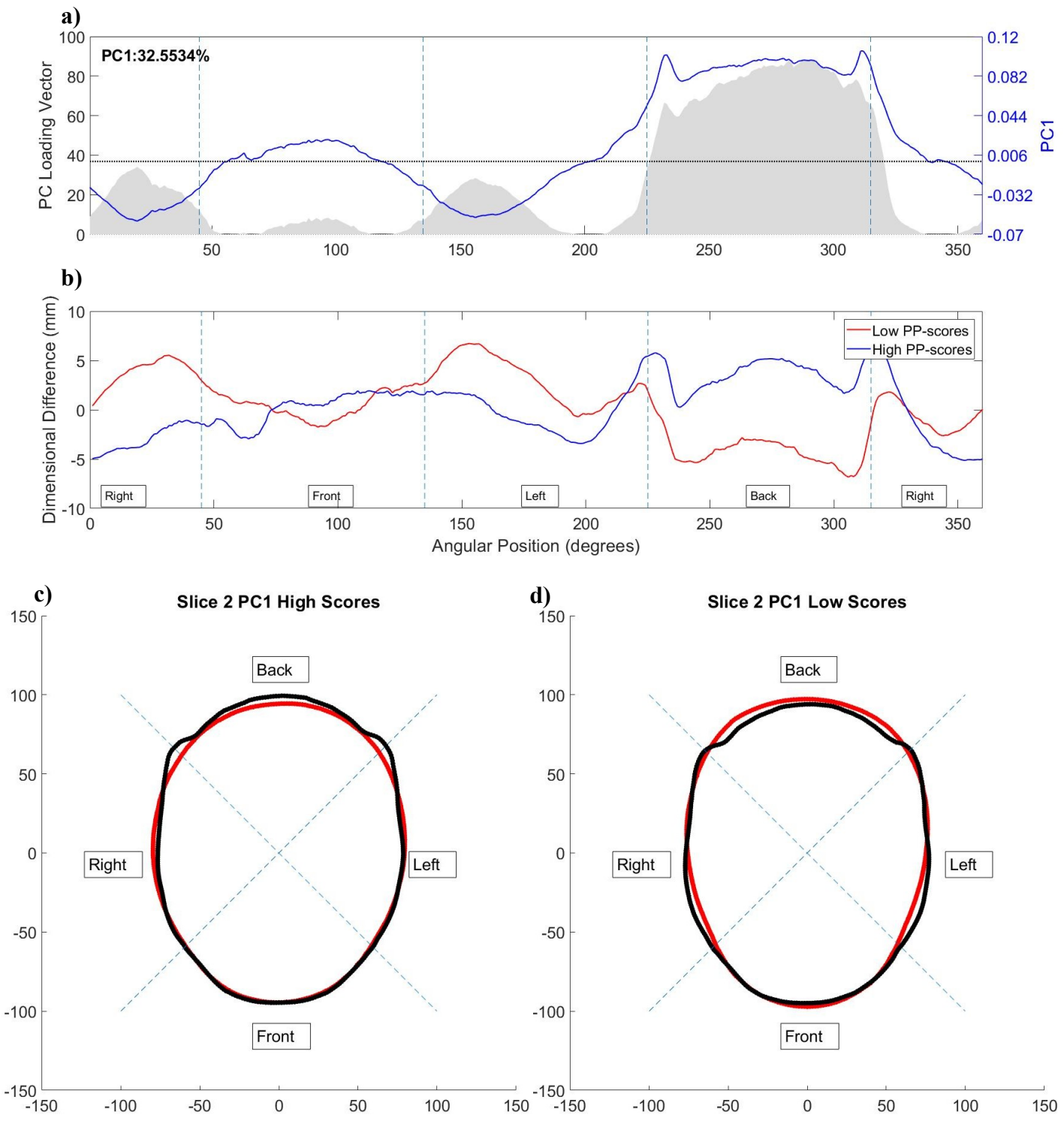


**Figure 8** Slice 2 Principal Component 1: a) eigenvector (PC1) represented in blue, variation in the principal component in grey; b) polar coordinate representations of 5<sup>th</sup> and 95<sup>th</sup> percentile PC1 scores; c) Cartesian representation of 95<sup>th</sup> percentile PC1 scores, red representing the outline of the head, black representing the outline of the helmet liner; d) Cartesian representation of 5<sup>th</sup> percentile PC1 scores, red representing the outline of the head, black representing the outline of the helmet liner.

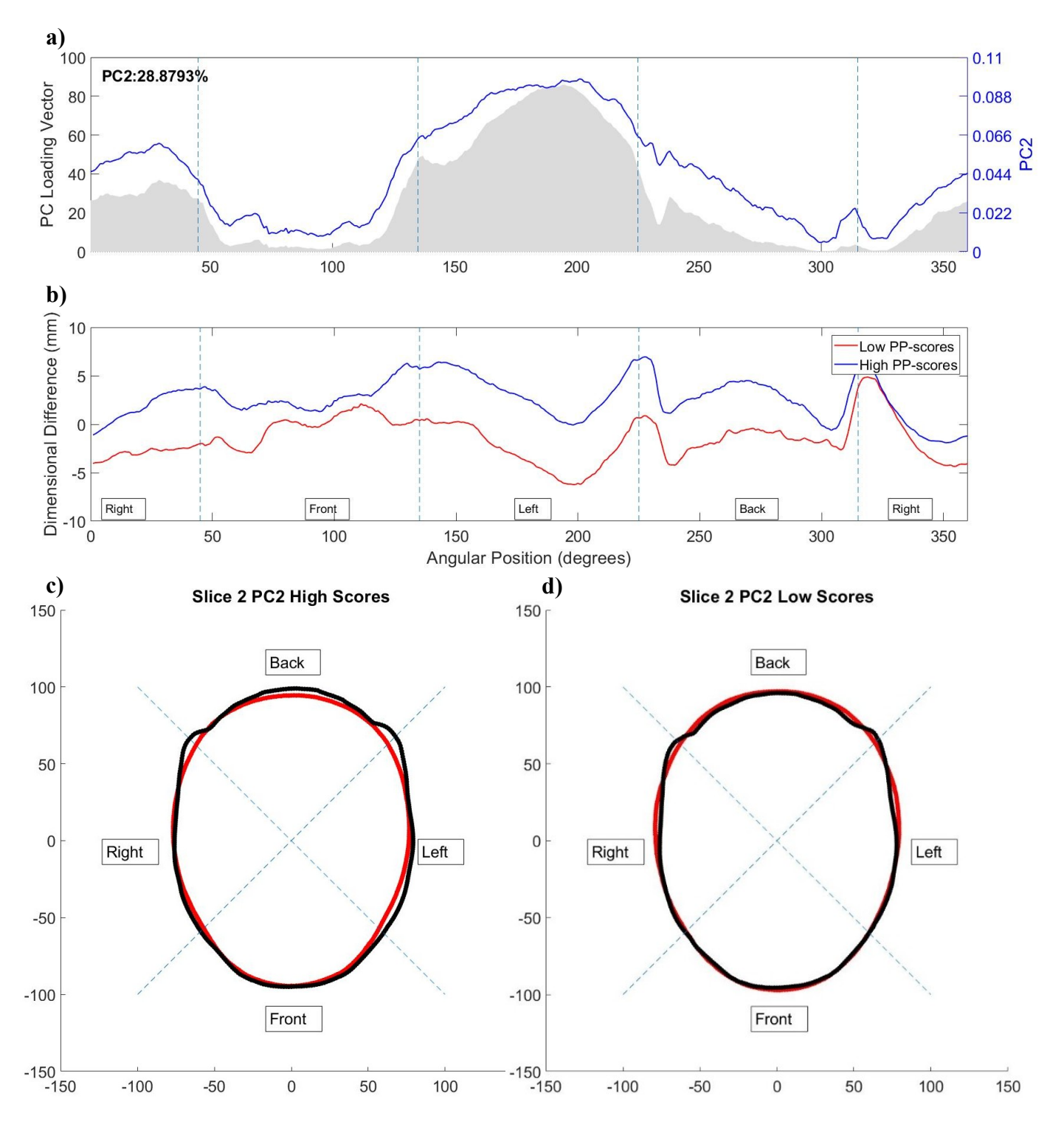


**Figure 9** Slice 2 Principal Component2: a) eigenvector (PC2) represented in blue, variation in the principal component in grey; b) polar coordinate representations of 5<sup>th</sup> and 95<sup>th</sup> percentile PC2 scores; c) Cartesian representation of 95<sup>th</sup> percentile PC2 scores, red representing the outline of the head, black representing the outline of the helmet liner; d) Cartesian representation of 5<sup>th</sup> percentile PC2 scores, red representing the outline of the head, black representing the outline of the helmet liner.

**Table 5** Pearson product-moment correlation coefficient for PC scores and head anthropometrics; shaded boxes denote statistical significance.

| Slice      | Circumference             | Length                  | Width                | L:W                        | cL:cW                     | ML Warp              | AP Warp                  |
|------------|---------------------------|-------------------------|----------------------|----------------------------|---------------------------|----------------------|--------------------------|
| 1          |                           |                         |                      | Ratio                      | Ratio                     |                      |                          |
| PC1        | r = -0.393,               | r=0.351,                | r=                   | r=0.780,                   | r=0.756,                  | r=                   | <i>r</i> =0.240,         |
|            | p<0.05                    | p>0.05                  | -0.847,              | p<0.001                    | p<0.001                   | -0.463,              | p>0.05                   |
|            |                           |                         | p<0.001              |                            |                           | p<0.005              |                          |
| PC2        | <i>r</i> = -0.108,        | r=                      | r=                   | r=0.029,                   | r= -0.0034,               | r=0.007,             | γ=                       |
|            | p>0.05                    | -0.071,                 | -0.084,              | p>0.05                     | p>0.05                    | p>0.05               | -0.441,                  |
|            |                           | p>0.05                  | p>0.05               |                            |                           |                      | p<0.005                  |
|            |                           |                         |                      |                            |                           |                      |                          |
| Slice      | Circumference             | Length                  | Width                | L:W                        | cL:cW                     | ML Warp              | AP Warp                  |
| Slice<br>2 | Circumference             | Length                  | Width                | L:W<br>Ratio               | cL:cW<br>Ratio            | ML Warp              | AP Warp                  |
|            | Circumference $r=0.273$ , | Length r=               | Width r= 0.497,      |                            |                           | ML Warp<br>r= 0.232, | AP Warp                  |
| 2          |                           |                         |                      | Ratio                      | Ratio                     | 1                    | 1                        |
| 2          | r= 0.273,                 | r=                      | r= 0.497,            | Ratio r=                   | Ratio<br>r= -0.393,       | r=0.232,             | r=                       |
| 2          | r= 0.273,                 | r=<br>-0.007,           | r= 0.497,            | Ratio r= -0.403,           | Ratio<br>r= -0.393,       | r=0.232,             | r=<br>-0.426,            |
| PC1        | r= 0.273,<br>p>0.05       | r=<br>-0.007,<br>p>0.05 | r= 0.497,<br>p<0.001 | Ratio<br>r= -0.403, p<0.01 | Ratio<br>r=-0.393, p<0.01 | r= 0.232,<br>p>0.05  | r=<br>-0.426,<br>p<0.005 |

## 3.4.4 M 5 Sub-Analysis

All three HFs were fitted with the medium sized helmet at its fifth adjustment setting in length (i.e. M\_5). To address the issue of helmet fit on HF versus HS, a focused analysis of all subjects wearing the helmet setting M\_5 (n=15) was completed. The anthropometrics of the M\_5 subjects and each HF are listed in Table 6. One sample t-tests were run, showing significant differences between the M\_5 subjects and each of the HFs in the mean circumference, length, compressed length, and width (p<0.001) (Table 7). The NOCSAE and CEN EN960 HFs were significantly less in mean compressed width than the M\_5 subjects (p<0.05). The length-to-width ratio of the NOCSAE HF was significantly greater than the mean of the M\_5 subjects (p<0.05). When taking the ratio of compressed length to compressed width, the CEN EN960 HF was significantly less than the M\_5 subjects (p<0.05). Lastly, in magnitude of anterior-posterior

warping, the Hybrid III was significantly greater than the mean of the  $M_5$  subjects (p<0.001), while the CEN EN960 was significantly less than the mean (p<0.01).

Comparing the entire subject HS sample to the M\_5 sample, similar measurements indicating significant difference from the HFs were observed, except for 1) the compressed width value of the CEN EN960 HF was significantly less than the M\_5 group; 2) the magnitude of medial-lateral warping was not significantly different than the M\_5 subjects; and 3) cL:cW ratio of the Hybrid III HF was not significantly different.

**Table 6** Anthropometrics of the M 5 subjects and the three different HFs (units in mm).

|   | M_5 Adult    |        | Hybrid | CEN   |
|---|--------------|--------|--------|-------|
|   | Subjects     | NOCSAE | III    | EN960 |
| Mean circumference (standard deviation) | 593.1 (6.7)  | 575    | 580    | 575   |
| Circumference minimum, maximum          | 583, 604     |        |        |       |
| Mean length (standard deviation)        | 208.5 (3.1)  | 200    | 201    | 199   |
| Mean compressed length (standard        |              |        |        |       |
| deviation)                              | 205.7 (3.7)  | 200    | 201    | 199   |
| Length minimum, maximum                 | 204, 212     |        |        |       |
| Compressed length minimum, maximum      | 199, 210     |        |        |       |
| Mean value of AP compression (standard  |              |        |        |       |
| deviation)                              | 2.8 (1.2)    | n/a    | n/a    | n/a   |
| Mean width (standard deviation)         | 163.0 (4.1)  | 153    | 156    | 155   |
| Mean compressed width (standard         |              |        |        |       |
| deviation)                              | 157.4 (3.8)  | 153    | 156    | 155   |
| Width minimum, maximum                  | 153, 169.5   |        |        |       |
| Compressed width minimum, maximum       | 149.5, 164.5 |        |        |       |
| Mean value of ML compression (standard  |              |        |        |       |
| deviation)                              | 5.6 (1.9)    | n/a    | n/a    | n/a   |
| Mean L:W (standard deviation)           | 1.28 (0.04)  | 1.31   | 1.29   | 1.28  |
| Mean cl:cW ratio (standard deviation)   | 1.31 (0.05)  | 1.31   | 1.29   | 1.28  |
| Length-to-width ratio minimum,          |              |        |        |       |
| maximum                                 | 1.2, 1.4     |        |        |       |
| Compressed length-to-compressed width   |              |        |        |       |
| ratio minimum, maximum                  | 1.2, 1.4     |        |        |       |
| Mean AP warping (standard deviation)    | 2.0 (0.04)   | 2      | 3.5    | 1     |
| AP warping minimum, maximum             | 0, 4         |        |        |       |
| Mean ML warping (standard deviation)    | 0.6 (1.2)    | 0.5    | 0.5    | 0     |
| ML warping minimum, maximum             | -0.5, 2.5    |        |        |       |

**Table 7** One sample t-test of measurements of subjects wearing M\_5 helmets, using HF measurements as the test value (estimated population mean): a) NOCSAE; b) Hybrid 3; c) CEN EN 960. Significant differences are denoted by asterisks.

a)

|              | Circumference | Length  | Compressed | Width   | Compressed | L:W    | cL:cW   | AP     | ML     |
|--------------|---------------|---------|------------|---------|------------|--------|---------|--------|--------|
|              |               |         | length     |         | width      | ratio  | ratio   | warp   | warp   |
| Mean of      | 593.1         | 208.5   | 205. 7     | 163.0   | 157.4      | 1.28   | 1.31    | 2.0    | 0.60   |
| Adult        |               |         |            |         |            |        |         |        |        |
| Subjects     |               |         |            |         |            |        |         |        |        |
| Standard     | 6.7           | 3.11    | 3.7        | 4.1     | 3.8        | 0.039  | 0.046   | 1.3    | 1.2    |
| deviation    |               |         |            |         |            |        |         |        |        |
| NOCSAE       | 575*          | 200*    | 200*       | 153*    | 153*       | 1.31*  | 1.31    | 2      | 0.5    |
| (test value) |               |         |            |         |            |        |         |        |        |
| t-statistic  | 10.488        | 10.582  | 6.016      | 9.539   | 4.474      | -2.963 | - 0.203 | 0.104  | 0.336  |
| Significance | p<0.001       | p<0.001 | p<0.001    | p<0.001 | p<0.01     | p<0.05 | p>0.05  | p>0.05 | p>0.05 |
| df           | 14            | 14      | 14         | 14      | 14         | 14     | 14      | 14     | 14     |

b)

|              | Circumference | Length  | Compressed | Width   | Compressed | L:W    | cL:cW  | AP warp | ML     |
|--------------|---------------|---------|------------|---------|------------|--------|--------|---------|--------|
|              |               |         | length     |         | width      | ratio  | ratio  |         | warp   |
| Mean of      | 593.1         | 208.5   | 205. 7     | 162.97  | 157.4      | 1.28   | 1.31   | 2.03    | 0.60   |
| Adult        |               |         |            |         |            |        |        |         |        |
| Subjects     |               |         |            |         |            |        |        |         |        |
| Standard     | 6.7           | 3.1     | 3.7        | 4.1     | 3.8        | 0.039  | 0.046  | 1.3     | 1.2    |
| deviation    |               |         |            |         |            |        |        |         |        |
| Hybrid III   | 580*          | 201*    | 201*       | 156*    | 156        | 1.29   | 1.29   | 3.5*    | 0.5    |
| (test value) |               |         |            |         |            |        |        |         |        |
| t-statistic  | 7.596         | 9.337   | 4.954      | 6.668   | 1.424      | -0.975 | 1.473  | -4.56   | 0.336  |
| Significance | p<0.001       | p<0.001 | P<0.001    | p<0.001 | p>0.05     | p>0.05 | p>0.05 | p<0.001 | p>0.05 |
| df           | 14            | 14      | 14         | 14      | 14         | 14     | 14     | 14      | 14     |

c)

|                           | Circumference | Length  | Compressed | Width   | Compressed | L:W    | cL:cW  | AP     | ML     |
|---------------------------|---------------|---------|------------|---------|------------|--------|--------|--------|--------|
|                           |               |         | length     |         | width      | ratio  | ratio  | warp   | warp   |
| Mean of<br>Adult          | 593.1         | 208.5   | 205. 7     | 163.0   | 157.4      | 1.28   | 1.31   | 2.0    | 0.60   |
| Subjects                  |               |         |            |         |            |        |        |        |        |
| Standard deviation        | 6.7           | 3.1     | 3.7        | 4.1     | 3.8        | 0.039  | 0.046  | 1.3    | 1.2    |
| CEN EN960<br>(test value) | 575*          | 199*    | 199*       | 155*    | 155*       | 1.28   | 1.28*  | 1*     | 0      |
| t-statistic               | 10.488        | 11.827  | 7.077      | 7.625   | 2.44       | 0.019  | 2.311  | 3.21   | 2.016  |
| Significance              | p<0.001       | p<0.001 | p<0.001    | p<0.001 | p<0.05     | p>0.05 | P<0.05 | p<0.01 | p>0.05 |
| df                        | 14            | 14      | 14         | 14      | 14         | 14     | 14     | 14     | 14     |

### 3.4.4.1 Helmet Dimensional Differences

The mean values of dimensional difference (DD) between helmet and head for the M\_5 subjects are listed in Table 8. The mean DD values of the M\_5 subjects were extracted from both Slice 1 and Slice 2. Subsequently, the mean, standard deviation, minimum, and maximum of the average DD values were determined for the M\_5 subjects. At Slice 1, the average DD value for the M\_5 subjects was negative (-1.79mm ±1.1 SD), indicating average compression at the headhelmet interface. Conversely, each of the HFs has positive average DD values, indicating net gapping (fig. 10). The mean DD values of each HF were significantly greater than those of the M\_5 subjects (p<0.001). At Slice 2, the average DD value of the M\_5 subjects was positive (0.59mm ± 1.2 SD), indicating average gapping at the head-helmet interface. The average DD values of the HFs were also positive, but were significantly greater in magnitude than the M\_5 subjects (p<0.05).

**Table 8** Mean DD values at Slice 1 and Slice 2 of the M 5 subjects (units in mm)

|                        | M_5 Subjects | NOCSAE              | Hybrid III | CEN EN960           |
|------------------------|--------------|---------------------|------------|---------------------|
| Slice 1 Mean DD (± SD) | -1.79 (1.1)  | 1.19*               | 0.58*      | 0.08*               |
|                        |              | (t=-10.155,         | (t=-8.075, | (t=-6.370,          |
|                        |              | p<0.001)            | p<0.001)   | p<0.001)            |
| Slice 1 DD minimum,    | -3.8, 1.2    |                     |            |                     |
| maximum                |              |                     |            |                     |
|                        |              |                     |            |                     |
| Slice 2 Mean DD        | 0.59 (1.2)   | 2.38*               | 1.39*      | 1.80*               |
| (standard deviation)   |              | ( <i>t</i> =-5.891, | (t=-2.627, | ( <i>t</i> =-3.979, |
|                        |              | p<0.001)            | p<0.05)    | p=0.001)            |
| Slice 2 DD minimum,    | -1.2, 2.5    |                     |            |                     |
| maximum                |              |                     |            |                     |
|                        |              |                     |            |                     |

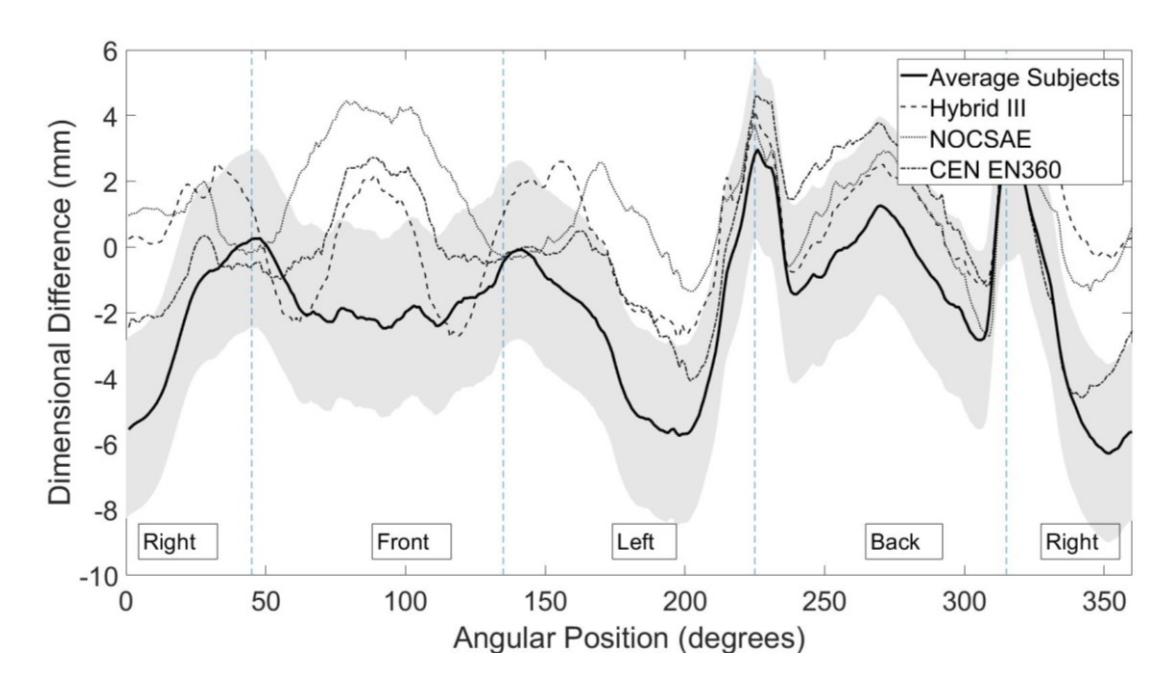


**Figure 10** Slice 1 DD of headforms and the mean of the M\_5 subjects in polar coordinates (standard deviation of M 5 subjects in grey).

### 3.4.4.2 Headform PC Ranks

From the original PCA models of the two slices, the PC scores of the M\_5 subjects, were extracted and ranked among the sub-sample. For the corresponding PCs, the PC scores of each HF were subsequently ranked within the subsample (Table 9).

In Slice 1 PC1, all HFs were ranked outside the median (ranks 6-10) of the M\_5 subjects, falling in the high end of the PC scores. The PC2 scores of the HFs were at the extreme high end, ranking higher than 93% to 100% of all M\_5 subjects. At Slice 2, the NOCSAE and Hybrid III HFs ranked within the median for PC1; the CEN EN960 HF had a high ranking score. All three HFs had PC scores ranked 12<sup>th</sup> or higher for PC2.

**Table 9** The ranks of each HF PC score for PCs 1 and 2.

|         | Headform     | PC1 | PC2 |
|---------|--------------|-----|-----|
| Slice 1 | NOCSAE M     | 14  | 15  |
|         | Hybrid III M | 14  | 14  |
|         | CEN EN960    | 11  | 15  |
| Slice 2 | NOCSAE M     | 6   | 15  |
|         | Hybrid III M | 10  | 12  |
|         | CEN EN960    | 13  | 12  |

### 3.5 Discussion

The objective of this study was to compare the quantitative hockey helmet fit between three different standard 50<sup>th</sup> percentile adult male HFs and a sample of adult males. Using the work of Greencorn [20] as a template, this goal was achieved. A sub-analysis was conducted, comparing each of the three HFs to the subjects wearing the helmet at the same adjustment as the HFs. The above results highlight discrepancies in helmet fit between the surrogate HFs and human wearers. The following sections will explore the limitations of headform-referenced landmarks for analysis and impact testing, as well as offer functional interpretations of the fit traits derived with regards to the incongruencies between headforms and human subjects.

### 3.5.1 Helmet referenced slice

The 2D head-helmet interface slices extracted from the 3D scanned models for analysis were defined using the helmet as a reference. This was an amendment to the study by Greencorn [20], which used the data points within a plane defined at 65mm superior to the Frankfurt Plane. At the anterior aspect of the model, the helmet slice was between 46.8 and 83.4mm (average 63.5mm ± 8.9SD) above the Frankfurt Plane. The use of a slice referenced to the helmet rather than the Frankfurt Plane for this study circumvented two primary issues: first, variability in the areas of the head and helmet captured by the slice due to differences in skull morphologies above the Frankfurt plane, and second, gaps in helmet coverage at the principal plane due to subjective

helmet orientation. The latter issue was found in 14 subjects (33%), where the bottom edge of the front of the helmet liner was not captured by the principal plane, indicating an absence of helmet coverage. This front gap likely occurred as a combination of the subject's head anthropometrics and preferences when wearing a helmet.

Further, using the helmet to reference the analyzed planes provided greater consistency for the data, as variability in head anthropometrics may affect the position of the principal plane relative to the helmet. For example, between subjects, the location of the principal plane (i.e. a fixed 65 mm above the Frankfurt plane) could vary tremendously as a percentage of the distance of cranial height, and relative to other cranial landmarks. Consequently, the intersection of the principal plane with the helmet would also be different between each subject. With dimensional difference as the measure of interest, the helmet-referenced slice standardized one of the variables used to calculate the DD. By extension, consideration should be taken to use this helmet referenced plane for identifying consistent helmet impact sites for standards testing.

# 3.5.2 Standard impact sites

The intersection of the headform based principal plane with the helmet varied greatly between standards and subjects. As a case example: the front boss impact site for hockey helmets used by the four standards associations is at "a point 25mm above the reference plane 45° in a clockwise direction from the anterior intersection of the median plane with the reference plane" [8]. The reference planes of ASTM, CEN, CSA, and ISO are specified at 60, 27.5, 27.5, and 29mm, respectively, above the Frankfurt Plane [47–50]. The lowest specified front boss impact site (CEN and CSA) is at 25mm above the reference plane, where the reference plane is 27.5mm above the Frankfurt Plane (i.e. 52.5mm above the Frankfurt Plane) [47,49]. While all three HFs had helmet coverage at this location, 18 subjects (43%) would not have coverage at this site.

This highlights insufficiencies of using head/headform-referenced landmarks for helmet impact sites, as HFs do not capture the different proportions of facial and cranial anthropometrics of people, nor do standards account for the subjective preferences of helmet users regarding helmet fit. Upon visual inspection, many subjects wore the helmet rotated off-centre, and with varying degrees of anterior-posterior helmet tilt. As the response of a helmet to impact may vary depending on the interaction at the head-helmet interface, further research is necessary to assess the effect of helmet fit on the protective properties of a helmet. Further, the above issues bring into question the veracity of extrapolating headform based reference impact sites.

### 3.5.3 Dimensional Differences

At both Slice 1 and Slice 2, the average DD values of each HF were greater than the average DD of all the HS. This corresponds with the significantly smaller HF dimensions measured compared to those of the HS. The superficial scalp tissues and hair of the head may account for some of the differences observed between HS and HF anthropometrics, as the current head-helmet alignment method considers only the exterior scanned surfaces. Thus, compressed caliper measures of head length and width were taken from HS to account for the compliance of superficial tissues. The combination of helmet warping, foam liner and scalp and hair compression would account for the negative DD values.

Another factor to be considered is the shape of HFs compared to the HS sample, with regards to congruence to helmet shape. The helmet used for the present study offered seven different length settings, for a total of +20mm of telescoping. Consequently, subjective preference of helmet tightness in the front and rear aspects of the head-helmet interface affected DD values in these regions. However, helmets were fitted to the HFs according to industry specifications, where the tightest allowable helmet adjustment was used on the HFs. Despite this, the front (70°-115°) and rear (240°-295°) DD values of the HFs (fig. 5a, b) indicate gapping; this

may be due to these regions of the HFs being flatter relative to the helmet, where the front and rear bosses delimit the contact in these regions.

# 3.5.4 Principal Component Analysis of Helmet-to-Head Fit: Dimension Differences Variance Explained

Following the work of Greencorn [20], PCA was used to describe fit by evaluating characteristics of the DD values around the full 360° circumference within each selected headhelmet plane. DD patterns of each PC were interpreted to identify specific fit traits. Two PCs were extracted from each slice, accounting for 66% of variance of Slice 1 and 61% of variance of Slice 2. PCs representing less than 15% of variance were not considered due to their low weight. PC score ranks of the HFs were compared to those of the HS, to assess fit characteristics of helmet-to-head and helmet-to-HF. For the 42 HS, a median PC score would have a rank between 15 and 28. As surrogate HFs are reported to represent a median 50<sup>th</sup> percentile adult male, it was expected the PC ranks of the HFs would fall within this median range. The ranking of the HFs relative to the HS will be elaborated in the following paragraphs.

Both Slice 1 PC1 and Slice 2 PC2 were interpreted to represent the medial-lateral warping of the helmet. Variability of these components arises from the interaction of lateral head surfaces with the relatively fixed width of the helmet. The combination of foam and scalp compression, as well as bowing out of the helmet shell, are thus required to allow for the accommodation of HS of differing head width. The helmet model used in this investigation, like most hockey helmets available for commercial sale, has telescopic settings allowing adjustment of helmet length but not width. Consequently, the extent of lateral warping allowed by helmet models to different head widths may be a determining factor for user preference and helmet sizing. In both slices, these PC scores were correlated with width, length-to-width ratio, and the magnitude of medial-lateral warping, and were all associated to the variability of medial-lateral

DD. For Slice 1 PC1, only the CEN EN960 HF had a PC score within the median HS range; however, both the Hybrid III and NOCSAE HFs had high scores, indicating less medial-lateral compression and helmet warping. Similarly, for Slice 2 PC2, the PC scores of all three HFs ranked higher than the median HS range, indicating greater gapping at the lateral aspects of the HF-helmet interface.

Slice 1 PC2 was interpreted to represent the anterior-posterior warping of the helmet, or fit relative to the selected helmet adjustment. These PC scores were negatively correlated with magnitude of anterior-posterior helmet warping. The alignment process may have anchored the front aspect of the helmet to the front aspect of the head, consequently presenting the DD variability of this PC in the rear aspect of the head-helmet interface. Despite the helmet's adjustable length, a certain degree helmet AP warping occurred. This illustrates the DD variability observed in this PC, as subjective preferences dictate loose versus tight fit in the anterior-posterior direction. However, the PC2 scores of the three HFs all ranked above the 95<sup>th</sup> percentile of HS scores, indicating an extreme high score. This likely corresponds with the gapping seen at the front and rear aspects of the HF-helmet interface (fig. 7a, b).

Slice 2 PC1 was interpreted to represent the general congruence of the head to the helmet liner. While the trace of the high scores of this PC show similar contours of head shape and the helmet liner, gapping at the rear aspect of the head-helmet interface should also be noted (fig 8c). This corresponds with the gapping of the HFs and the helmet liner at the rear of the helmet (fig 5b). The PC score ranks of the HFs for Slice 2 PC1 reflect the degree of gapping, where the NOCSAE HF demonstrated the greatest magnitude of gapping in the rear region and had a very high PC score. The CEN EN960 and Hybrid III HFs demonstrated less gapping in the rear region, and have PC scores ranking within or just above the median HS range.

### 3.5.5 M 5 Sub-analysis

In addition to comparing the helmet fit of the HFs with the entire sample of HS, a subanalysis was completed for subjects wearing the same helmet setting as the HFs. All three HFs
were fitted to the medium sized helmet at the fifth length setting (M\_5); the sub-analysis
included the 15 subjects who wore the helmet at the M\_5 adjustment. It was expected the
anthropometrics of the M\_5 sub-group would demonstrate similarities to the anthropometrics of
the HFs, but this was not the case. All three HFs were significantly less than the M\_5 subjects in
the following measures: circumference, length, compressed length, width. Two out of three HFs
(NOCSAE and CEN EN960) were significantly less than the M\_5 subjects in compressed width.
Only the NOCSAE HF was significantly greater than the mean length-to-width ratio of the M\_5
subjects, and only the CEN EN960 HF was significantly less than the mean M\_5 subjects'
compressed length-compressed-width ratio.

With regards to the magnitude of anterior-posterior warping, the Hybrid III HF was significantly greater and CEN EN960 HF was significantly less than the mean of the M\_5 subjects. The magnitude of medial-lateral warping was not significantly different between M\_5 subjects and the HFs. This may be attributed to properties of the helmet, specifically the lack of medial-lateral "give" permitted by the helmet, suggesting width as the limiting dimension of helmet sizing.

Between the entire HS sample and the M\_5 sub-group, measurements of significant difference from the HFs were largely the same between groups. Comparing the distribution PC score ranks of the HFs within the full HS sample and the M\_5 sample reveal much similarity. The categorization of HF PC score ranks into the median, high, or very high ranges were generally consistent between the two groups. This highlights two related findings: first, helmets fit the HFs differently than they do the HS; and second, the HFs are poor analogues of human

heads. As seen in the M\_5 sub-analysis, the HFs do not represent the heads of subjects wearing the helmet at the same adjustment. The similarities in the high HF PC score ranks between both the HS and M\_5 groups indicate the incongruence between the shape of HFs and human subjects, and consequently discrepancies in helmet fit between the HFs and subjects.

### 3.5.6 Implications

The incongruence in helmet fit between the HFs and HS is noteworthy due to its potential consequences on helmet impact attenuation properties. Helmet fit has been demonstrated to affect the protection conferred by a helmet to the user [12]. As helmets are certified for commercial sale based on the results of standard impact testing on helmets mounted on HFs, it is unknown whether these certified helmets provide users of different head shape with the same level of protection. The helmet-to-head and helmet-to-headform fit discrepancy may be an important factor to consider when assessing head injury prevention in ice hockey.

### 3.5.7 Limitations

The cumulative errors in this 3D shape analysis of helmet-to-head fit were primarily the sum of rendering and alignment errors. Base on the suggestions by Greencorn [20], a reference ruler was securely attached to the subject during scanning, improving the scaling calibration accuracy.

A two-camera system (replacing the prior one-camera approach by Greencorn [20]) was implemented to improve the speed of data collection and to reduce motion artifact of the subject. This reduced RMSE error form 1.14mm to 0.40mm. Despite these protocol improvements, some subject scans were unusable: either the head model or the intermediate model came out poorly (i.e. facial features were smudged, or 3D artifacts appeared on the model). This may be due to motion artifacts between pictures from the participant and/or the cameras. A setup with three or

more synchronized cameras at different perspective angle positions would reduce the occurrence of failed scans.

The resolution of the models was limited by the ceiling placed by AutoDesk® ReCap<sup>TM</sup> on the number of photos that could be used to render each model. The software limited the free educational license to 100 photos per model. With a full ReCap<sup>TM</sup> Photo license, models can be created with up to 1000 photos. This license has an annual fee over \$1000, in addition to the cost of "cloud credits", where 12 to 55 are charged per 3D model rendered based on the number of photos.

Alignments of helmet and head models to the intermediate model were done manually, resulting in error (average RMSE = 0.40mm). Automation of this process through landmark or vertex recognition would reduce processing time and eliminate human error.

This study delimited both the helmet and human subject point clouds as rigid. The outer helmet shell and inner foam liner both warp to accommodate head shapes. Additionally, hair, skin, and musculature overlaying the cranium all permit compression. While the current method provides insight into the helmet-to-head fit, further refinement to account for interaction of hair and scalp compression with the helmet liners is needed.

### 3.5.8 Future Directions

This study delimited analysis of geometric fit to two 2D head planes of male subjects and surrogate HFs. The logical next steps would be to expand the analysis to describe and compare the fit of ice hockey helmets for males, females, and children, and to use 3D PCA and more advanced techniques such as Procrustes 3D shape analysis [19] and applied functional data analysis [64] to determine a more global understanding of helmet fit. Furthermore, as helmet fit between human subjects and surrogate headforms differed, by extension, helmet impact function may too be expected to differ. Consequently, the helmet's performance on standard impact tests

may be different than its response to impact during real-world use. Future research should consider analyzing the different impact responses of a hockey helmet when fitted to different head shapes. Further, this may establish a quantitative relationship between fit and helmet protectiveness.

### 3.6 Conclusion

This study compared the fit of a hockey helmet on standard HFs and human subjects. Substantial discrepancies in helmet fit metrics (i.e. DD, PCA) were observed between the HFs and HS. This raises the question of the external validity of using standard headforms to represent a normal range of human head shapes for assessing helmet-head impact responses.

# 3.7 Acknowledgements

The authors would like to thank Charles-Antoine Desrochers and Donald Nault, Bauer Hockey Ltd, for assisting with data collection.

# 4. Conclusions

This study compared the fit of a hockey helmet on standard HFs and human subjects.

Substantial discrepancies in helmet fit metrics (i.e. DD, PCA) were observed between the HFs and HS. This raises the question of the external validity of using standard headforms to represent a normal range of human head shapes for assessing helmet-head impact responses.

### 5. References

- 1. Kelly KD, Lissel HL, Rowe BH, Vincenten J a, Voaklander DC. Sport and recreation-related head injuries treated in the emergency department. Clin J Sport Med. 2001;11(2):77–81.
- 2. Emery C, Kang J, Shrier I, Goulet C, Hagel B, Benson B, et al. Emery et al. Can Med Assoc J. 2011;183(11):1249–56.
- 3. Agel J, Dick R, Nelson B, Marshall SW, Dompier TP. Descriptive epidemiology of collegiate women's ice hockey injuries: National Collegiate Athletic Association injury surveillance system, 2000-2001 through 2003-2004. J Athl Train. 2007;42(2):249–54.
- 4. Agel J, Dompier TP, Dick R, Marshall SW. Descriptive epidemiology of collegiate men's ice hockey injuries: National Collegiate Athletic Association injury surveillance system, 1988-1989 through 2003-2004. J Athl Train. 2007;42(2):241–8.
- 5. Clement, L, Jones D. Research and development of hockey protective equipment: A historical perspective. Saf Ice Hockey Philadelphia, Am Soc Test Mater. 1989;164–86.
- 6. CSA. Z262.1-09 Ice hockey helmets. Can Stand Assoc. 2009;
- 7. ASTM. F1045-07 Standard performance specification for ice hockey helmets. 2007;
- 8. Pearsall DJ, Wall RE, Hoshizaki BT. Comparison of International Safety Standards for Ice Hockey Helmets. 2000;
- 9. Hoshizaki TB, Brien SE, Bailes JE, Maroon JC, Kaye AH, Cantu RC. The science and design of head protection in sport. Neurosurgery. 2004.
- 10. Forero Rueda MA, Cui L, Gilchrist MD. Finite element modelling of equestrian helmet impacts exposes the need to address rotational kinematics in future helmet designs. Comput Methods Biomech Biomed Engin [Internet]. 2011;14(12):1021–31. Available from: http://www.tandfonline.com/doi/abs/10.1080/10255842.2010.504922
- 11. Rowson S, Duma SM, Beckwith JG, Chu JJ, Greenwald RM, Crisco JJ, et al. Rotational head kinematics in football impacts: An injury risk function for concussion. Ann Biomed Eng. 2012;40(1):1–13.
- 12. Chang L-T, Chang C-H, Chang G-L. Fit Effect of Motorcycle Helmet. A Finite Element Modeling. Vol. 44, JSME International Journal Series A. 2001. p. 185–92.
- 13. Cobb BR, Macalister A, Young TJ, Kemper AR, Rowson S, Duma SM. Quantitative comparison of Hybrid III and National Operating Committee on Standards for Athletic Equipment headform shape characteristics and implications on football helmet fit. Proc Inst Mech Eng Part P J Sport Eng Technol. 2015;229(1):39–46.
- 14. Hubbard RP, McLeod DG. A Basis for Crash Dummy Skull and Head Geometry. In: Human Impact Response [Internet]. 1973. p. 129–52. Available from: http://link.springer.com/10.1007/978-1-4757-1502-6 7
- 15. Hodgson V. National Operating Committee on Standards for Athletic Equipment football helmet certification program. Medicine and science in sports; 1975. p. 225–32.
- 16. Daniels G. The Average Man. No TN-WCRD-53-7 AIR FORCE Aerosp Med Res LAB WRIGHT-PATTERSON AFB OH. 1952;
- 17. Liu K, Greencorn D, Aponte D, Robbins S, Pearsall D. Comparison of Hockey Helmet Fit from an Adult Male Sample and Standard Human Headforms Using 3D Modeling. In: ASB2017. Boulder; 2017. p. 115–6.
- 18. Ellena T, Subic A, Mustafa H, Pang TY. The helmet fit index an intelligent tool for fit assessment and design customisation. Appl Ergon [Internet]. 2016;55:194–207. Available from: http://dx.doi.org/10.1016/j.apergo.2016.02.008

- 19. Ball R, Shu C, Xi P, Rioux M, Luximon Y, Molenbroek J. A comparison between Chinese and Caucasian head shapes. Appl Ergon. 2010;41(6):832–9.
- 20. Greencorn D. Ice Hockey Helmet Fit Using 3D Modeling. McGill Masters Thesis. 2017;
- 21. Luo Y, Liang Z. Sport helmet design and virtual impact test by image-based finite element modeling. Conf Proc . Annu Int Conf IEEE Eng Med Biol Soc IEEE Eng Med Biol Soc Annu Conf. 2013;
- 22. McCrory P, Meeuwisse W, Johnston K, Dvorak J, Aubry M, Molloy M, et al. Consensus statement on Concussion in Sport—The 3rd International Conference on Concussion in Sport held in Zurich, November 2008. J Sci Med Sport [Internet]. 2009;12:340–51. Available from: www.sciencedirect.com
- 23. Daneshvar DH, Nowinski CJ, Mckee AC, Cantu RC. The Epidemiology of Sport-Related Concussion. Clin Sports Med [Internet]. 2011;30(1):1–17. Available from: http://dx.doi.org/10.1016/j.csm.2010.08.006
- 24. Purcell L, Carson J. Sport-related concussion in pediatric athletes. Clin Pediatr (Phila). 2008;47(2):106–13.
- 25. McCrea M, Hammeke T, Olsen G, Leo P, Guskiewicz K. Unreported concussion in high school football players: implications for prevention. Clin J Sport Med [Internet]. 2004;14(1):13–7. Available from: http://www.ncbi.nlm.nih.gov/entrez/query.fcgi?cmd=Retrieve&db=PubMed&dopt=Citati on&list\_uids=14712161%5Cn/citations?view\_op=view\_citation&continue=/scholar%3Fh l%3Den%26start%3D10%26as\_sdt%3D0,39%26scilib%3D1&citilm=1&citation\_for\_view=IzT9eFEAAAAJ:IjCSPb-
- 26. Delaney JS, Lacroix VJ, Gagne C, Antoniou J. Concussions among university football and soccer players: A pilot study. Clin J Sport Med. 2001;11(4):234–40.
- 27. Cantu RC, Voy R. Second impact syndrome: a risk in any contact sport. Phys Sportsmed. 1995;23(6):27–34.
- 28. Mueller FO. Catastrophic Head Injuries in High School and Collegiate Sports. J Athl Train. 2001;36(3):312–5.
- 29. Langlois JA, Rutland-Brown W, Wald MM. The Epidemiology and Impact of Traumatic Brain Injury A Brief Overview. J Head Trauma Rehabil. 2006;21(5):375–8.
- 30. Halstead ME, Walter KD. Sport-Related Concussion in Children and Adolescents. Pediatrics [Internet]. 2010;126(3):597–615. Available from: http://pediatrics.aappublications.org/cgi/doi/10.1542/peds.2010-2005
- 31. Patel DR, Reddy V. Sport-related Concussion in Adolescents. Vol. 57, Pediatric Clinics of North America. 2010. p. 649–70.
- 32. Emery CA, Meeuwisse WH. Injury Rates, Risk Factors, and Mechanisms of Injury in Minor Hockey. Am J Sports Med [Internet]. 2006;34(12):1960–9. Available from: http://ajs.sagepub.com/lookup/doi/10.1177/0363546506290061
- 33. McKeever C, Schatz P. Current Issues in the Identification, Assessment, and Management of Concussions in Sports-Related Injuries. Appl Neuropsychol. 2003;10(1):4–11.
- 34. Field M, Collins MW, Lovell MR, Maroon J. Does age play a role in recovery from sports-related concussion? A comparison of high school and collegiate athletes. J Pediatr. 2003;142(5):546–53.
- 35. Pellman EJ, Lovell MR, Viano DC, Casson IR. Concussion in professional football: Recovery of NFL and high school athletes assessed by computerized neuropsychological testing Part 12. Neurosurgery. 2006;58(2):263–72.

- 36. Zhang L, Yang KH, King AI. A Proposed Injury Threshold for Mild Traumatic Brain Injury. J Biomech Eng [Internet]. 2004;126(2):226. Available from: http://biomechanical.asmedigitalcollection.asme.org/article.aspx?articleid=1411575
- 37. Gennarelli TA, Thibault LE, Adams JH, Graham DI, Thompson CJ, Marcincin RP. Diffuse axonal injury and traumatic coma in the primate. Ann Neurol. 1982;12(6):564–74.
- 38. Bain AC, Meaney DF. Tissue-Level Thresholds for Axonal Damage in an Experimental Model of Central Nervous System White Matter Injury. J Biomech Eng [Internet]. 2000;122(6):615. Available from: http://biomechanical.asmedigitalcollection.asme.org/article.aspx?articleid=1404429
- 39. Kleiven S. Evaluation of head injury criteria using a finite element model validated against experiments on localized brain motion, intracerebral acceleration, and intracranial pressure. Int J Crashworthiness. 2006;11(1):65–79.
- 40. Rousseau P, Post A, Hoshizaki TB. A Comparison of Peak Linear and Angular Headform Accelerations Using Ice Hockey Helmets. 2009;6(1):1–11.
- 41. Miltz J, Ramon O. Energy absorption characteristics of polymeric foams used as cushioning materials. Polym Eng Sci. 1990;30(2):129–33.
- 42. Gimbel G, Hoshizaki T. Compressive properties of helmet materials subjected to dynamic impact loading of various energies. Eur J Sport Sci. 2008;8(6):341–9.
- 43. Landro L Di, Sala G, Olivieri D. Deformation mechanisms and energy absorption of polystyrene foams for protective helmets. 2002;21:217–28.
- 44. Gurdjian E, Roberts V, Thomas L. Tolerance curves of acceleration and intracranial pressure and protective index in experimental head injury. J Trauma. 1966;6(5):600–4.
- 45. Gadd CW. Use of a Weighted-Impulse Criterion for Estimating Injury Hazard. In: SAE Technical Paper [Internet]. 1966. p. 164–74. Available from: http://papers.sae.org/660793/
- 46. Versace J. A Review of the Severity Index. SAE Technical Paper. 1971.
- 47. Canadian Standards Association (CSA). Ice hockey helmets. 2015;
- 48. ASTM. F1045-16 Standard Performance Specification for Ice Hockey Helmets. Current. 2016;1–10.
- 49. CEN. Protective equipment for use in ice hockey Part 1: General requirements (ISO 10256-1:2016). 2016;
- 50. 10256-2:2016 I. Protective equipment for use in ice hockey -- Part 2: Head protection for skaters. 2016;
- 51. Hoshizaki TB, Post A, Oeur RA, Brien SE. Current and future concepts in helmet and sports injury prevention. Neurosurgery. 2014;75:S136–48.
- 52. Rowson B, Rowson S, Duma SM. Hockey STAR: A Methodology for Assessing the Biomechanical Performance of Hockey Helmets. Ann Biomed Eng. 2015;43(10):2429–43.
- 53. Mustafa H, Pang TY, Perret-Ellena T, Subic A. Impact attenuation of customized user-centered bicycle helmet design. Procedia Eng [Internet]. 2015;112:77–84. Available from: http://dx.doi.org/10.1016/j.proeng.2015.07.179
- 54. Pheasant S, Halsgrave C. Bodyspace: Anthropometry, Ergonomics and the Design of Work. 3rd ed. CRC Press; 2016.
- 55. Cavalcanti M, Rocha S, Vannier M. Craniofacial measurements based on 3D-CT volume rendering: implications for clinical applications. Dentomaxillofacial Radiol. 2004;33(3):170–6.
- 56. Collins D, Neelin P, Peters T, Evans A. Automatic 3D intersubject registration of MR

- volumetric data in standardized Talairach space. J Comput Assist Tomogr. 1994;18(2):192–205.
- 57. Meunier P, Tack D, Ricci A, Bossi L, Angel H. Helmet accommodation analysis using 3D laser scanning. Appl Ergon. 2000;31:361–9.
- 58. Ball R. 3-D Design Tools from the SizeChina Project. Ergon Des. 2009;17(3):8–13.
- 59. Schaaf H, Pons-Kuehnemann J, Malik C, Streckbein P, Preuss M, Howaldt H, et al. Accuracy of three-dimensional photogrammetric images in non-synostotic cranial deformities. Neuropediatrics. 2010;41(1):24–9.
- 60. Lerma JL, Navarro S, Cabrelles M, Villaverde V. Terrestrial laser scanning and close range photogrammetry for 3D archaeological documentation: the Upper Palaeolithic Cave of Parpalló as a case study. J Archaeol Sci. 2010;37(3):499–507.
- 61. Remondino F, Barazzetti L, Nex F, Scaioni M, Sarazzi D. UAV photogrammetry for mapping and 3d modeling–current status and future perspectives. Int Arch Photogramm Remote Sens Spat Inf Sci [Internet]. 2011;38–1/C22(1):25–31. Available from: http://www.zenit-sa.com/
- 62. MacAlister A. Surrogate Head Forms for the Evaluation of Head Injury Risk. Brain Inj Biomech [Internet]. 2013; Available from: http://vtechworks.lib.vt.edu/handle/10919/23818
- 63. Robbins SM, Astephen Wilson JL, Rutherford DJ, Hubley-Kozey CL. Reliability of principal components and discrete parameters of knee angle and moment gait waveforms in individuals with moderate knee osteoarthritis. Gait Posture. 2013;38(3):421–7.
- 64. Ramsay J, Silverman B. Applied functional data analysis: methods and case studies. Springer; 2007.

# 6. Appendices

| Appendix A: Consent form Statement of Consent  |  |
|--|--|
| I,, AGREE  | TO VOLUNTARILY PARTICIPATE IN THE STUDY                    |
| DESCRIBED ABOVE ABOUT 3D ANALYSIS OF ICE HOCKEY  | Y HELMET FIT.  |
| I HAVE RECEIVED AND READ A DETAILED DESCRIPTION SATISFIED WITH THE EXPLANATIONS THAT WERE GIRESEARCH PROJECT, INCLUDING THE POTENTIAL PARTICIPATION IN THIS STUDY. | VEN TO ME REGARDING THE NATURE OF THIS                     |
| I am aware that I have the right to withdraw my cons without any prejudices.   | ent and discontinue my participation at any time           |
| I consent and wish to receive a private URL link to my 3   | D model. YES / NO  |
| (only those with access to the link may view the files)  | email:   |
| I consent that the lab use my 3D head model for prese I understand that I will be identifiable.  | ntations, demonstrations, and in other lab media. YES / NO |
| SUBJECT  |  |
| (Signature)  | (Print name)   |
| RESEARCHER   |  |
| (Signature)  | (Print name)   |
| Date:  |  |

### INFORMATION AND CONSENT DOCUMENT

# **3D Analysis of Ice Hockey Helmet Fit**

Investigators: Daniel Aponte, Ph.D. Candidate (Kinesiology, daniel.aponte@mail.mcgill.ca)

Kristie Liu, M.Sc. Student (Kinesiology, kristie.liu@mail.mcgill.ca)

**Supervisor:** David Pearsall, Ph.D (david.pearsall@mail.mcgill.ca)

Biomechanics Laboratory, Department of Kinesiology and Physical Education, McGill

University

#### Statement of Invitation:

You are invited to participate in a research project conducted by the above named investigators. This research project will be performed at the IHRG laboratory (Room 400, 475 avenue des Pins Ouest, Montreal, QC, Canada, H2W 1S4). You will be entered into a lottery with a 1 in 20 chance to win a \$50 gift card, as well as receiving a 3D file of your scanned head for your participation. You are asked to come to one experimental session that will last approximately 30 minutes. We greatly appreciate your interest in our work.

### **Purpose of the Study**

The purpose of this study is to determine the ideal fit parameters of ice hockey helmets, and generate a database of hockey players head to improve the fit and comfort of hockey helmets. This study will also compare the dimensions and shape of human heads to that of crash dummy heads used in testing and certification of hockey helmets.

### Your participation in this study involves:

- 1. Providing informed consent prior to the experimental session
- Providing data concerning your physical attributes, hockey experience, and hockey equipment usage (e.g., height, age, number of years playing ice hockey, highest level played, current helmet model, etc.)
- 3. Being photographed for the 3D models, and filling out a fit and comfort questionnaire.

### **Risks and Discomforts**

It is anticipated that you will encounter no significant discomfort during these experiments. There is minimal risk associated with these experiments.

### **Benefits**

You will receive compensation for your participation in the form of a 3D file of your head scan and a 1 in 20 chance to win a \$50 gift card. Benefits of this study may lead to a new helmet fitting system and a better understanding of the geometrical fit of hockey helmets on different head shapes.

### **Photographs**

The technique used to build a 3D model of your head requires that we take multiple photographs of you at many different angles. These photographs will only be used to build 3D models of your head, and will not be used for any other purpose, or disseminated from this laboratory. The 3D model of your head may (with your express consent) be used in poster and conference presentations, lab media and demonstrations. Due to the accuracy of the 3D model, you will be identifiable.

### Confidentiality

All the personal information collected during the study you concerning will be encoded in order to keep their confidentiality. These records will be maintained at the Biomechanics Laboratory by Dr. David Pearsall for 7 years after the end of the project, and will be destroyed upon the expiration of this time frame. Only members of the research team will be able to access them. In case of presentation, your personal information will remain completely anonymous.

### **Dissemination of Results**

The results of the study will be disseminated through an MSc thesis (Greencorn), PhD thesis (Aponte), journal publications and conference posters (if applicable), and in a formal report to Bauer Hockey Corp.

### **Sources of Funding**

Currently, this study is funded by an NSERC Collaborative Research and Development Grant, in collaboration with the Bauer Hockey Corporation.

### **Inquiries Concerning this Study**

If you require information concerning the study (experimental procedures or other details), please do not hesitate to contact Daniel Aponte or David Greencorn at the address listed at the top of this document.

### **Responsibility Clause**

In accepting to participate in this study, you will not relinquish any of your rights and you will not liberate the researchers nor their sponsors or the institutions involved from any of their legal or professional obligations.

#### Consent

Please be advised that your participation in this research undertaking is strictly on a voluntary basis, and you may withdraw at any time.

A copy of this form will be given to you before the end of the experimental session.

| Appendix B: Participant Demographics and Participant: | Anthropometrics  Date: |  |  |  |  |
|---|------------------------|--|--|--|--|
| Participant   | Information            |  |  |  |  |
| Participant   | Information            |  |  |  |  |
| Age   |                        |  |  |  |  |
| Highest Level Played                                  |                        |  |  |  |  |
| Years of Experience                                   |                        |  |  |  |  |
| Their Current Helmet Model                            |                        |  |  |  |  |
| Their Current Helmet Size                             |                        |  |  |  |  |
| Their Current Helmet Colour                           |                        |  |  |  |  |
| Email address (if applicable)                         |                        |  |  |  |  |
| Anthrop  Head Circumference (mm)                      | oometrics              |  |  |  |  |
| A/P head length (mm)                                  |                        |  |  |  |  |
| A/P head compression (mm)                             |                        |  |  |  |  |
| M/L head width (mm)                                   |                        |  |  |  |  |
| M/L head compression (mm)                             |                        |  |  |  |  |
|   |                        |  |  |  |  |
|   |                        |  |  |  |  |
| Helmet Data   |                        |  |  |  |  |
| Size and Adjustment                                   |                        |  |  |  |  |
| A/P bucking   |                        |  |  |  |  |
| M/L buckling  |                        |  |  |  |  |
|   |                        |  |  |  |  |

# **Appendix C: Helmet Fit Questionnaire**

| Participant: _ |                          | Date: |             |  |  |
|----------------|--------------------------|-------|-------------|--|--|
|                | Helmet Fit Questionnaire |       |             |  |  |
|                | Order:                   | Size: | Adjustment: |  |  |

| Fit - Circle one of each                              |              |       |                   |         |                   |       |              |
|---|--------------|-------|-------------------|---------|-------------------|-------|--------------|
| Overall Helmet Fit                                    | Too<br>Loose | Loose | Slightly<br>Loose | Perfect | Slightly<br>Tight | Tight | Too<br>Tight |
| Helmet Width Fit                                      | Too<br>Loose | Loose | Slightly<br>Loose | Perfect | Slightly<br>Tight | Tight | Too<br>Tight |
| Helmet Length Fit                                     | Too<br>Loose | Loose | Slightly<br>Loose | Perfect | Slightly<br>Tight | Tight | Too<br>Tight |
| Comfort   1 = Very Poor, 4 = Neutral, 7 = Very Good   |              |       |                   |         |                   |       |              |
| Overall Comfort                                       | 1            | 2     | 3                 | 4       | 5                 | 6     | 7            |
| Front Comfort   | 1            | 2     | 3                 | 4       | 5                 | 6     | 7            |
| Back Comfort  | 1            | 2     | 3                 | 4       | 5                 | 6     | 7            |
| Side Comfort (R)                                      | 1            | 2     | 3                 | 4       | 5                 | 6     | 7            |
| Side Comfort (L)                                      | 1            | 2     | 3                 | 4       | 5                 | 6     | 7            |
| Stability   1 = Very Poor, 4 = Neutral, 7 = Very Good |              |       |                   |         |                   |       |              |
| Overall Stability                                     | 1            | 2     | 3                 | 4       | 5                 | 6     | 7            |
| Front/Back Stability                                  | 1            | 2     | 3                 | 4       | 5                 | 6     | 7            |
| Side/Side Stability                                   | 1            | 2     | 3                 | 4       | 5                 | 6     | 7            |
| Safety   1 = Very Poor, 4 = Neutral, 7 = Very Good    |              |       |                   |         |                   |       |              |
| Perceived Safety                                      | 1            | 2     | 3                 | 4       | 5                 | 6     | 7            |

